A&A 392, 33–52 (2002)
DOI: 10.1051/0004-6361:20020877

Astronomy & Astrophysics

Shakhbazian compact galaxy groups

I. Photometric, spectroscopic and X-ray study of ShCG 154, ShCG 166, ShCG 328, ShCG 360

H. Tiersch[1,⋆], H. M. Tovmassian[2], D. Stoll[1], A. S. Amirkhanian[3], S. Neizvestny[4], H. Böhringer[5], and H. T. MacGillivray[6]

[1] Sternwarte Königsleiten, 81477 München, Leimbachstr. 1a, Germany
[2] Instituto Nacional de Astrofísica Optica y Electrónica, Apartado Postal 51 y 216, CP 72000, Puebla, Pue., México
e-mail: hrant@inaoep.mx
[3] Byurakan Astrophysical Observatory, NAS, Armenia
e-mail: vachik@nssp-gov.am
[4] Special Astrophysical Observatory, RAS, Nizhny Arkhyz, Russia
e-mail: neiz@sao.ru
[5] MPI Extraterrestrische Physik, Garching, Germany
e-mail: hxb@mpe.mpg.de
[6] Royal Observatory, Edinburg, UK
e-mail: hmg@roe.ac.uk

Received 3 September 2001 / Accepted 18 April 2002

Abstract. Shakhbazian compact galaxy groups belong to the interesting class of compact groups. Because of their large number (the catalogue contains 377 entries) we are able to study the groups in different stages of evolution. Here we give the results of detailed study of four groups, ShCG 154, ShCG 166, ShCG 328 and ShCG 360. We present the redshifts of individual galaxies in groups, the results of the surface photometry in *BVR*, the contourplots of the surface brightness versus effective radius of galaxies, the twisting postion angle versus effective radius of galaxies, the radial velocity dispersions, the crossing times, the mass-to-luminosity ratios of groups and the results of the X-ray study. The dynamical state of groups, interactions between member galaxies, and the physical parameters of groups are discussed.

Key words. galaxies: clusters: general – galaxies: interactions – galaxies: kinematics and dynamics – galaxies: photometry – X-rays: galaxies

1. Introduction

Compared with galaxy clusters, compact groups (CGs) are relatively rare. The first lists of CGs were compiled three-four decades ago (Vorontsov-Velyaminov 1959; Arp 1966; Rose 1977; Duus & Newell 1977; Geller & Huchra 1983). The largest list of CGs was compiled by Shakhbazian, Petrosian, Baier and Tiersch from 1973–1979 with the results of a systematic search of more than 200 POSS prints. The list contains 377 groups published in 10 compilations (Shakhbazian 1973; Shakhbazian & Petrosian 1974; Baier et al. 1974; Petrosian 1974, 1978; Baier & Tiersch 1975, 1976a, 1976b, 1978, 1979).

The interest in CGs increased greatly when *N*-body simulations showed that CGs must undergo strong dynamical evolution over relatively short time scales ($\sim 10^9$ years), resulting in a coalescence to one giant elliptical galaxy (e.g. Barnes 1985, 1989; Mamon 1986; Bode et al. 1993). It followed that signs of dynamical friction, tidal interaction between galaxies, and galaxy merging should be observed in CGs.

Contrary to the widely studied HCGs (e.g. Hickson et al. 1989a, 1989b, 1992; Hickson 1993), Shakhbazian Compact galaxy Groups (ShCGs) have not been intensively investigated. The redshifts of only a few groups have been measured until recently (Robinson & Wampler 1973; Arp et al. 1973; Mirzoyan et al. 1975; Kirshner & Malamuth 1980; Amirkhanian 1987; Kodaira et al. 1988, 1990; Kodaira & Sekiguchi 1991; Lynds et al. 1990; del Olmo & Moles 1991; Tiersch et al. 1995a, 1995b, 1995c, 1996a, 1999a, 1999b), the morphology of galaxies in a few groups was studied by Amirkhanian & Egikian (1987), Bettoni & Fasano (1995) and Tiersch et al. (1995c).

A few years ago we commenced an observational study of ShCGs, aiming to throw more light on the subject. ShCGs are a relatively homogeneous sample, identified according to the following criteria: groups consist of generally 5–15 members; the apparent magnitudes of individual galaxies are generally

Send offprint requests to: H. Tiersch, e-mail: htiersch@uni.de

⋆ Visiting Astronomer, German-Spanish Astronomical Centre, Calar Alto, operated by the Max-Plank-Institute for Astronomy, Heidelberg, jointly with the Spanish National Commission for Astronomy.

between 14^m and 19^m; the distances between galaxies are typically 3–5 times the diameter of galaxies; nearly all group galaxies are extremely red, there are at most 1–2 blue galaxies in a group; members of groups are compact (relatively high surface brightness, borders not diffuse)[1].

In the original papers the positions of groups were given with relatively low accuracy. To study the groups in detail the correct positions of member galaxies have been determined (Stoll et al. 1993a, 1993b, 1994a, 1994b, 1996a, 1996b, 1996c, 1997a, 1997b, 1997c).

The knowledge of the correct positions of member galaxies of ShCGs allowed Oleak et al. (1995, 1998) to investigate the apparent ellipticity of about 300 ShCGs using the method proposed by Rood (1979). It was found that the mean apparent axial ratio[2] $b/a \sim 0.5$. Assuming a random orientation of groups in space, the true intrinsic axial ratio distribution, best represented by a simple Gaussian intrinsic distribution of prolate spheroids with

$$< b/a >_{\rm intr} \; = \; < q > \; = \; 0.3 \quad \text{and} \quad \sigma = \pm 0.15,$$

was deduced. Hence, the ellipticities of ShCGs are higher than that of rich clusters of galaxies (DiFazio & Flin 1988) and that of elliptical galaxies (see e.g. Binggeli 1982). They are objects with the highest ellipticities and a "cigar"-like space configuration. This result provided strong confirmation of the reality of ShCGs, since in the case of chance line-of-sight alignments of field galaxies we would expect much higher axial ratios.

Tovmassian & Tiersch (2001) found that faint galaxies in the environment of ShCGs, as in the case of HCGs (Tovmassian 2001), are distributed along the elongation of the corresponding group, and most probably rotate together with the group members around the common gravitational center. Hence, ShCGs as HCGs (Tovmassian 2001), are, possibly, more stable formations than has been predicted by N-body simulations. Nevertheless, processes of interaction are very likely in such elongated systems, in spite of the suggested regular rotation of member galaxies around the gravitational centers of corresponding groups. Therefore, these groups are good laboratories for the study of a galaxy-galaxy interaction and related phenomena.

In this paper we present the results of the spectroscopy and direct imaging of member galaxies in the four groups ShCG 154, ShCG 166, ShCG 328 and ShCG 360, and discuss the obtained results. For three of these groups, X-ray emission was detected.

2. Observations and results

The coordinates of the centers of the studied groups are given in Table 1. The extinctions, Q_B, (Schlegel et al. 1998) valid for the region of each group with sizes of about 5′, are given as well.

[1] Later observations, including this one, made with high angular resolution, revealed that member galaxies are mostly ordinary E and S0 galaxies.

[2] a is the distance between the most widely separated galaxies, and b is the sum of the shortest distances from a to the most distant galaxy on either side of a.

Table 1. Positions of groups ShCG 154, 166, 328, and 360, and extinction Q_B.

ShCG	α (2000)	δ (2000)	Q_B [mag]
154	$11^h22^m54^s$	+01°06′52″	0.16
166	$16^h52^m48^s$	+81°37′54″	0.29
328	$14^h20^m31^s$	−09°20′21″	0.23
360	$15^h41^m26^s$	+04°43′56″	0.27

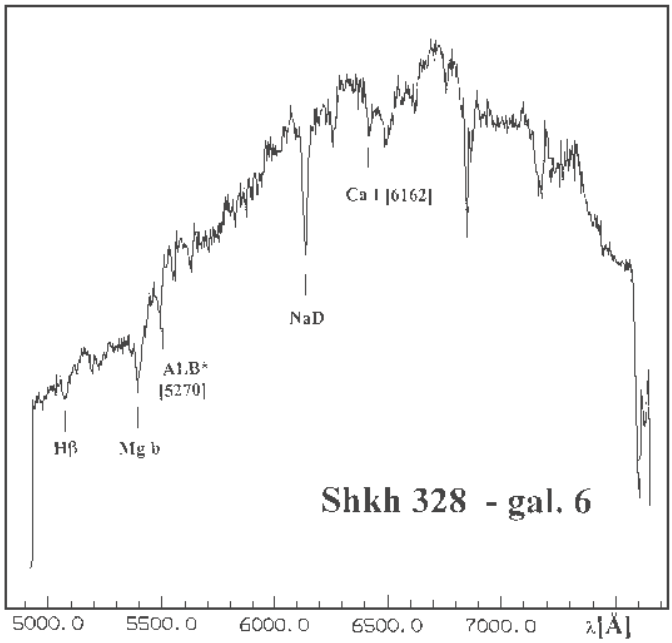

Fig. 1. The spectrum of galaxy 6 in ShCG 328.

2.1. Spectroscopy

Spectroscopic observations of 28 galaxies in the studied four groups were made with the Cassegrain spectrograph of the 2.2 m telescope of the DSAZ Calar Alto. The spectrograph is fitted with a TEK CCD with 1024 × 1024 pixels (24 μm squared) and a 600 lines/mm grating blazed at 5000 Å with a dispersion of 120 Å/mm for the wavelength range of 4900–7650 Å. Because of the faintness of the observed galaxies, the slit width was set at ∼2.5″. The wavelengths were calibrated using a HeAr comparison spectrum taken before and after each galaxy esposure, and the pixel-to-pixel variation of the CCD was calibrated using dome flats. The spectra of galaxies were obtained with an integration time of 60 min; the signal-to-noise ratio is normally about 20. The spectra resemble those of K-type stars. A typical example, galaxy 6 in ShCG 328, is shown in Fig. 1. Absorption features of Hβ, MgIb and NaD were generally identified. For determination of redshifts the MIDAS package (*standard reduction – long* and *standard reduction – spec* with programs therein) was used. The errors were estimated using the cross-correlation technique (Tonry & Davis 1979). The accuracy of the measured radial velocities (RV) is between 40 km s^{-1} and 60 km s^{-1} depending on the sharpness and the number of the measured spectral lines. The uncertainties in the case of relatively low signal-to-noise

Table 2. The radial velocity of member galaxies in the groups ShCG 154, 166, 328, and 360.

ShCG 154			ShCG 166			ShCG 328			ShCG 360		
g	v [km s^{-1}]	δv [km s^{-1}]	g	v [km s^{-1}]	δv [km s^{-1}]	g	v [km s^{-1}]	δv [km s^{-1}]	g	v [km s^{-1}]	δv [km s^{-1}]
1	21 620	±45	1	11 497	±39	1	12 931	±75	1	33 051	±49
2	21 985	±48	2	11 740	±43	2	13 590	±55	2	33 201	±54
3	21 751	±56	3	12 046	±51	3	14 220	±52	3	31 612	±53
7	22 753	±55	4	12 040	±57	4	14 100	±61	4	31 852	±60
9	21 599	±61	5	11 626	±64	6	13 530	±45	5	31 642	±64
10	20 492	±81	6	11 740	±76	8	13 590	±83	9	31 882	±72
			7	12 349	±64				11	32 871	±79
			8	12 531	±71				14	31 852	±44

ratio do not exceed 80 km s^{-1}. The *RV*s have been corrected for solar motion according $\Delta v = 300 \sin l^{\rm II} \cdot \cos b^{\rm II}$ km s^{-1}. The radial velocities of individual galaxies and the corresponding errors of measurements are given in Table 2.

2.2. Direct imaging and photometry

We obtained high-resolution images of the four studied groups in B, V, and R. Observations were made during two observing runs in 1993 and 1994 in the RC focus of the 1.23 m telescope at the DSAZ Calar Alto, Spain. The TEK CCD detector with 512×512 pixels of 27 μm squared giving a sky coverage of $4'\,50'' \times 4'\,50''$ with an image scale of 0.565″/pxl was used. Observations were made at seeing conditions better than 2″. In total 46 galaxies were photometried in *BVR*.

The images were processed with the MIDAS image processing package. The night sky was eliminated by means of a software program developed by Shergin and Kniazev at SAO, Russia. This program takes into account the complicated conditions in a CG with overlapping galaxy halos. The *BVR* magnitudes were calibrated in the Kron/Cousins photometric system using the standard star cluster M 67. The K corrections were neglected since the groups are relatively nearby.

In the case of isolated images of galaxies the outer isophotes in all three colours sometimes reach values fainter than $\mu = 26\overset{\rm m}{.}5$/arcsec^2. The *BVR* magnitudes are estimated, however, till the $\mu = 26\overset{\rm m}{.}5$/arcsec^2 surface brightness. The limiting surface brightness of galaxies with images of halos superimposed on halos of other galaxies does not reach this value. Such galaxies were sliced to the disturbed and to the undisturbed parts, and the galaxy magnitude was calculated by a special MIDAS program that fits the elliptical isophotes using the undisturbed part of the galaxy. This is a reasonable technique, provided the galaxies have retained their symmetry despite overlapping. If a galaxy is embedded in a common halo, then the last undisturbed isophote (brighter than $\mu = 26\overset{\rm m}{.}5$/arcsec^2) determines the magnitude.

The estimated accuracy of magnitudes is generally about $0\overset{\rm m}{.}06$. In the case of images embedded in a common envelope, the error could be somewhat worse. The measured magnitudes were corrected for the extinction, Q_B, within our Galaxy (according to Schlegel et al. 1998). The inner individual extinction within spiral galaxies is estimated according to $A_i = 0.72 \log (1/\cos i)$. The inclination angle i is deduced by a procedure in MIDAS. The extinction in V and R are calculated by $E_{B-V} = 0.238 Q_B$ and $E_{V-R} = 0.590 Q_B$, respectively.

The diameters, axial ratios and the position angles of major axis of galaxies are deduced normally from the $26\overset{\rm m}{.}5$/arcsec^2 isophotes. In the case of galaxies with overlapping halos we used the outermost fitted ellipse and extrapolated the surface brightness profile down to the local background.

ShCGs are, on average, at least by ∼3 times farther than HCGs (Tiersch et al. 1996b; Tovmassian et al. 1999). The member galaxies in ShCGs are correspondingly fainter and have smaller angular sizes. Bettoni & Fasano (1995) studied the morphology of early type galaxies in a sample of ShCGs with relatively bright members, and mentioned that the luminosity and geometrical profiles had in general low spatial resolution and relevant noise. For this reason we did not deduce and discuss the boxiness, since, as Lima Neto & Combes (1993) showed by N-body simulations, the galaxies formed by a sequence of mergers display few signs of boxiness. This conclusion was confirmed by Bettoni & Fasano (1993, 1995) and Fasano & Bettoni (1994), who found that early-type galaxies in compact groups seem to show less boxiness than galaxies in other environments.

For determination of morphological types of the observed galaxies we used the luminosity profiles of the surface brightness (in R), μ, versus the effective radius, $r^n_{\rm eff}$. The effective radius $r_{\rm eff} = (a + b)/2$, where a and b are the major and the minor half axis of the corresponding isophote determined by the MIDAS ellipses fitting procedure. Galaxies with a spheroidal bulge generally obey the $r^{1/4}$ law (Schombert 1987). They are classified as of E/S0 type. If the luminosity profile follows the $1/r$ law, the corresponding galaxy is classified as a spiral. However, as it was mentioned by Pildis et al. (1995), any deviations from ellipticity in both the core and envelope, as well as deviations from concentric ellipses and an $r^{1/4}$ law in the envelope are observed. Often, these features imply that a galaxy has undergone an earlier interaction, but not in every case is this true. In some cases the ellipticals tend to have outer envelopes that are brighter than the predictions of an $r^{1/4}$ law and so the deviations must be interpreted with restraint. Comparison of

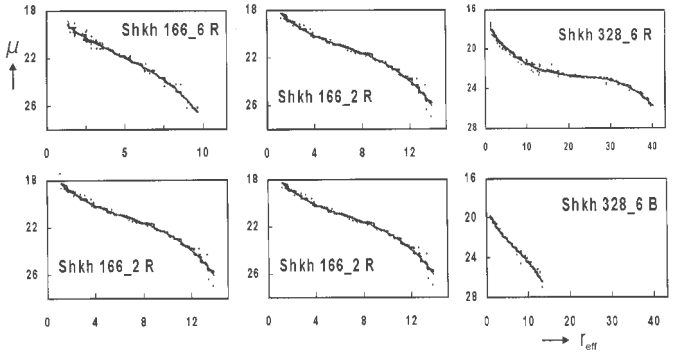

Fig. 2. An example of the surface brightness, μ, vs. effective radius, $r_{\rm eff}$, for a spiral (ShCG 166-6), an E/S0 (ShCG 166-2), and an elliptical with heated halo (ShCG 328-6) in B and R.

the luminosity profiles $\mu - r_{\rm eff}$ in different colours also helps to determine the morphological type of a galaxy. In a spiral galaxy the luminosity profile in B continues smoothly much farther, while in R it bends relatively close to the center of a galaxy (e.g. galaxy ShCG 166-6, Fig. 2). The luminosity profiles in V are very similar to those in R. In an elliptical galaxy (galaxy ShCG 166-2, Fig. 2) the luminosity profile in R, on the contrary, continues to the border of an elliptical galaxy, while in B it bends nearer to the center of a galaxy. The very large radius of the galaxy ShCG 328-6 (third panel in Fig. 2) in R in comparison to the very small radius in B is evidence of a dynamically heated halo of an elliptical galaxy. For determination of the morphological types we inspected also the images of galaxies.

The photographs in R and the isophotes of the studied groups ShCG 154, ShCG 166, ShCG 328 and ShCG 360 are presented in Figs. 3, 7, 10 and 13, respectively[3]. Each image is a superposition of three frames of 30 min exposure time. The isolines are chosen arbitrarily to reveal the outer faintest regions of galaxies, generally not seen on direct images. In all images north is up and east is left. The galaxy identification numbers stem from the original publications (Petrosian 1974, 1978; Baier & Tiersch 1978). The $\mu - r_{\rm eff}^{1/4}$ profiles of the surface brightness in R versus effective radius for galaxies in the four groups studied are presented in Figs. 5, 8, 11, and 14, respectively. Depending on the brightness of the galaxy and presence of a bright nearby neighbour, the limiting surface brightness is different. The radii until which the curves are drawn are also different, ranging from ~4″ to more than 10″. The spread of the measured surface brightness becomes sufficiently large at the faint limits of the curves. The drawn curves are the best fits of the measured points.

Additionally we investigated the phenomenon of isophotal twisting in early-type galaxies of the Shakhbazian groups. This twisting of the isophotes has been interpreted as a signature of mutual tidal perturbations or galaxy collisions (di Tullio 1979; Kormendy 1982). The twisting profiles, α, vs. the radius, $r^{1/4}$, of the individual galaxies of the four Shakhbazian groups are plotted in Figs. 6, 9, 12, and 15.

[3] The groups in the figures are marked as Shkh according to old designation.

The results of the photometry of member galaxies in the studied groups are presented in Tables 4–7. In these tables the following information is given: Col. 1 – the galaxy identification number, Col. 2 – the magnitude in $B_{26.5}$, Col. 3 – the axial ratio, b/a, in B, Col. 4 – the diameter of the galaxy out to the surface brightness of $26\overset{\rm m}{.}5$/arcsec^2 in B; Cols. 5–7 – the latter three parameters in V; Cols. 8–10 – the same parameters in R; Col. 11 – the position angle of the major axis, α, in R; Col. 12 – the inclination, i (in R); Col. 13 – the galaxy type.

ShCG 154 was observed also with the UK Schmidt telescope, using a film with the fine-grain Eastman-Kodak 4415 emulsion. Four images in the R passband, with a scale of 67.14″/mm were obtained with 1 hour exposure time. The films were digitized on the COSMOS high-speed measuring machine. The plot shown in Fig. 4 is the result of digital summation of four films. Here the extended halos as well as the intergalactic background are clearly seen.

2.3. The X-ray observations

All four ShCGs were investigated for X-ray emission with the ROSAT satellite that is well suited for the study of galaxy groups because of its high sensitivity, low background and reasonable spatial resolution.

ShCG 328 was observed in the mode of pointed observations of the ROSAT PSPC from July 15 to August 9, 1993. The image frame of ShCG 328 is the sum of 9 time-integrations between 700 s and 2600 s with a total exposure of 11 022 s. The X-ray data for ShCG 154 and ShCG 360 are taken from the ROSAT PSPC All Sky Survey archive. Due to scanning of the sky by the ROSAT telescope in great circles in the plane orthogonal to the solar direction, the exposure time is different in different parts of sky. The exposure time of ShCG 154 was 430 s and that of for ShCG 360 was 500 s.

The reduction of the data was made using the method described by Mahdavi et al. (1997). The observed area was divided into a grid, then the number of counts in each cell was estimated. The cells around the source were used to determine the background counts. Poisson statistics gives the background noise. The statistical significance of a detection is then σ = (background-subtracted counts of the source)/(background noise). For the three groups, found to be X-ray emitters, the significance $\sigma > 3$.

The X-ray emission of ShCGs cannot be resolved into emission of individual sources because the PSPC has a $FWHM$ of 25″, while the distances between galaxies in groups are generally smaller. Hence, it was impossible to separate diffuse extended emission from the emission of individual galaxies. However, the question of whether the observed X-ray emission is the integral emission of individual sources within the group or the extended emission of intragroup gas can be answered by a comparison of the X-ray luminosity being typical for hot intracluster gas within a galaxy group with the integrated X-ray luminosity of individual objects within a group. The latter is usually much smaller.

The X-ray emission was detected from ShCG 154, ShCG 328 and ShCG 360, and for ShCG 166 it was below

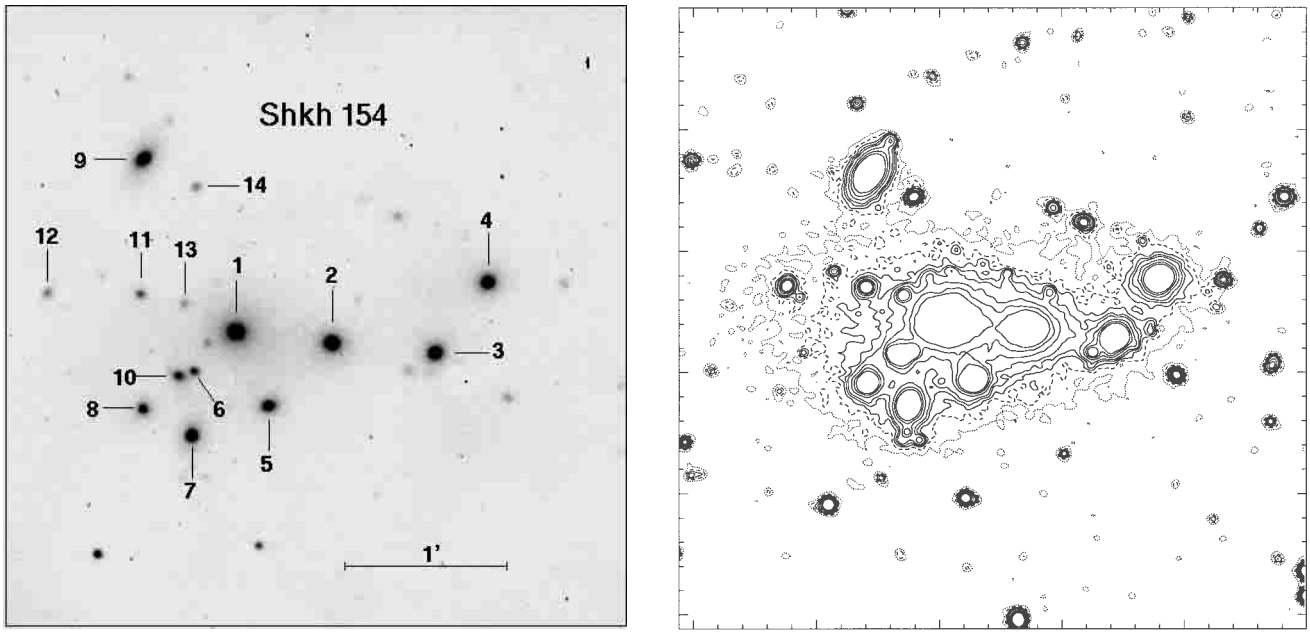

Fig. 3. The photograph of ShCG 154 in *R* (left) and the isophotal contour plot of galaxies (right).

Table 3. The ROSAT PSPC data for ShCG 154, ShCG 328 and ShCG 360.

ShCG	cts	exp	cts	n_H	L_X
				10^{20}	10^{42}
		[s]	[s^{-1}]	[cm^{-2}]	[erg s^{-1}]
154	31 ± 6	430	0.07	5.0	13.8 ± 6
328	107 ± 10	11 022	0.01	6.1	1.3 ± 0.3
360	57 ± 8	500	0.11	3.8	82.2 ± 16

the detection limit determined by the local background, ~30 counts per 16 arcsec^2. The radial extent of the X-ray emission in all three groups is over 1′. Since the point-spread function of the PSPC falls to less than 10^{-3} of its central value for a radius greater than 1′ (Hasinger et al. 1992), the PSF does not affect the radial extent of the emission. The contour maps of the extended (background subtracted) X-ray emission of ShCG 154, ShCG 328, and ShCG 360 in arbitrary units are presented in Figs. 17–19. The results of the X-ray observations are given in Table 3, in which the following information is given: Col. 1 – the ShCG number, Col. 2 – the background-subtracted counts in the range 0.4–2.4 keV, Col. 3 – the exposure time, Col. 4 – the background-subtracted group count rate in cts s^{-1}, Col. 5 – the column density of hydrogen (see Schlegel et al. 1998), n_H, Col. 6 – the X-ray luminosity. L_X, calculated by assuming that the metalicity is half of the solar abundance.

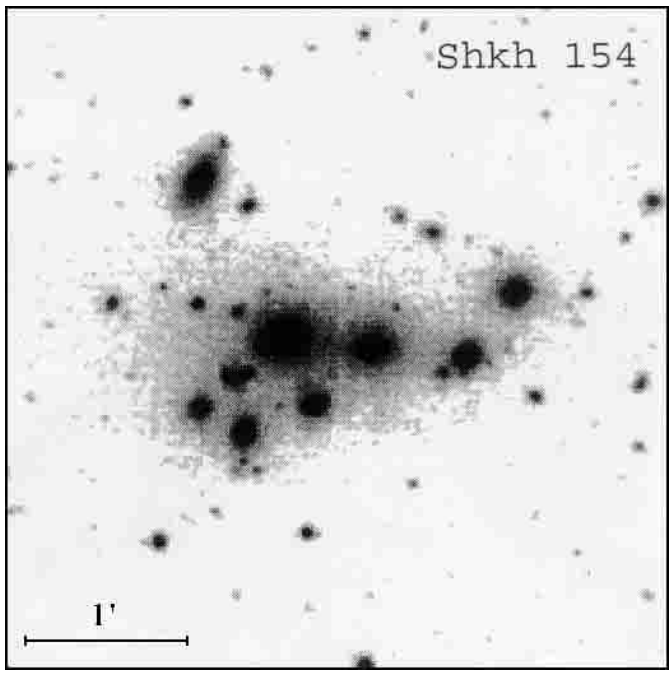

Fig. 4. The image of ShCG 154 obtained with the UK Schmidt.

3. Discussion

It is assumed (Hickson et al. 1992) that a galaxy is a member of a CG if its *RV* does not differ from the mean *RV* of the group by more than $\Delta v \sim 1000$ km s^{-1}. The measured *RV*s of galaxies (Table 2) show that all galaxies included in the original lists of the studied four ShCGs, with possibly one exception, belong to corresponding groups. Hence, although not all members of groups are spectroscopically investigated, the groups are regarded as real physical formations.

The redshifts, z, of the four ShCGs cover the range from 0.04 to 0.11, i.e., they all are located beyond the Local Supercluster, and are farther than the Coma cluster (z = 0.0202).

The space density of galaxies in ShCGs is much higher than in galaxy clusters. This may result in formation of extended optical halos around galaxies by tidal "heating" and, consequently, may cause diffuse light in the group potential. One has

Table 4. Photometric parameters of galaxies in ShCG 154.

$g-xy$	B			V			R					type
	m	b/a	D [″]	m	b/a	D [″]	m	b/a	D [″]	α [°]	i [°]	
1	17.59	0.9	16	16.30	0.9	17	15.51	1.0	22	68	22	E/S0
2	17.88	0.9	12	16.60	0.7	13	15.80	0.8	18	−88	28	S0
3	18.04	0.8	10	16.90	0.9	10	16.15	0.9	14	−26	25	S0/Sa
4	18.14	0.9	8	16.98	0.9	9	16.04	0.9	12	−73	21	S0
5	18.63	0.9	11	17.13	0.9	11	16.46	0.8	17	−69	25	S0/Sa
6	19.64	0.9	4	18.98	0.9	5	18.20	0.9	5	−8	23	E/S0
7	18.30	0.8	9	16.95	0.8	12	16.30	0.7	12	−10	33	S0
8	19.04	0.9	7	17.78	0.9	9	17.26	0.9	9	71	26	S0
9	17.96	0.6	12	16.67	0.6	13	15.94	0.6	13	−30	44	S0/Sa
10	19.53	0.9	8	18.08	0.8	9	17.44	0.8	10	21	20	S0/Sa
11	19.97	0.8	6	18.96	0.8	7	18.40	0.8	7	49	19	E/S0
12	20.25	0.6	6	19.58	0.7	6	18.76	0.9	8	−30	31	S0/Sa
13	20.98	0.9	5	19.75	0.8	6	19.00	0.8	7	−53	27	S0
14	20.48	0.8	5	19.65	0.7	5	18.90	0.7	6	−36	30	E/S0

to be cautious, however. Since galaxies in ShCGs are often very close to each other on the sky, their overlapping isophotes may create an impression of bridges. Hence, a subtle approach in the argumentation is needed.

3.1. ShCG 154

Radial velocities are measured for six out of eight brightest members. Five of them have accordant redshifts. The *RV* of galaxy 10 differs from the mean value by ∼1400 km s^{-1}.

The group is clearly an interacting one. The countour plot of the group (the right panel of Fig. 3) shows that the common halo, in which at least seven galaxies are embedded, is sufficiently enlarged, which is a sign of interaction. The large halo in which all these galaxies are embedded is more impressive in the deep UK Schmidt image (Fig. 4). The isophotes of the halos of the two brightest galaxies, 1 and 2, are distended at their closest separation. The halo of galaxy 5 is extended towards the dominant galaxy 1. Galaxies 7 and 8 seem to have slightly extended halos. Hence, they may also be involved in the interaction. Two other relatively bright galaxies of the group, 3 and 4, interact with each other, and, perhaps, also with the central concentration of galaxies. The extension of the halo of galaxy 4 towards the central group is a hint of this. Moreover, the halos of these two galaxies are larger in comparison with that of undisturbed brighter galaxy 9 (see Table 4) at the north-east of the group. Galaxies 6 and 10, embedded in the common halo, may be projected over the central concentration. The redshifts of both galaxies differ appreciably from the mean redshift of four other galaxies.

Galaxies 11, 12, and 14 are out of the central large halo, and are not involved in interaction. Galaxy 13 may just be projected over the large halo. The *RV*s of the last four galaxies are not measured, hence their membership of the group is not yet confirmed. There are a number of other faint objects in the area of the group. They seem to "surround" the two brightest galaxies of the group.

The $\mu - r_{\rm eff}^{1/4}$ profiles of the surface brightness in R versus effective radius for galaxies in the studied group are presented in Fig. 5. Provided the disturbation of the twisting curves is caused by environmental effects, the α vs. $r^{1/4}$ – curves of the galaxies 1, 2, 8, and 13 (see Fig. 6) hint at a strong galaxy-galaxy interaction.

3.2. ShCG 166

This group is very elongated and consists of three luminous galaxies and a few fainter objects. The radial velocities of eight of them are measured (Table 2). The bright galaxies within this not-so-dense group show no apparent interaction with each other (Fig. 7). However, galaxies 2 and 3 are in interaction with their nearby neighbours. Galaxy 3 demonstrates some signs of dynamical distortion. Its halo is extended (compare with that of the brighter, undisturbed galaxy 1), and is apparently interacting with galaxy 11. The latter seems to be "swallowed" by galaxy 3, while galaxy 10 seems to be projected over the extended halo of galaxy 3. The contour plot (right panel of Fig. 7) shows that galaxy 11 does not have any halo. It obviously is disrupted by the bright and massive galaxy 3, and we see its bare nucleus. Comparison of galaxy 2 with the much brighter galaxy 1 shows that the halo of the former is extended, which apparently may be caused by interaction with galaxies 5 and 6.

Two galaxies, 6 and 10, may be spirals. They are classified as S0/Sa. The other 6 photometried galaxies are of S0 or E types.

The $\mu - r_{\rm eff}^{1/4}$ profiles of the surface brightness in R versus effective radius for galaxies in the studied group are presented in Fig. 8. The twisting curves α vs. $r^{1/4}$ are seen in Fig. 9.

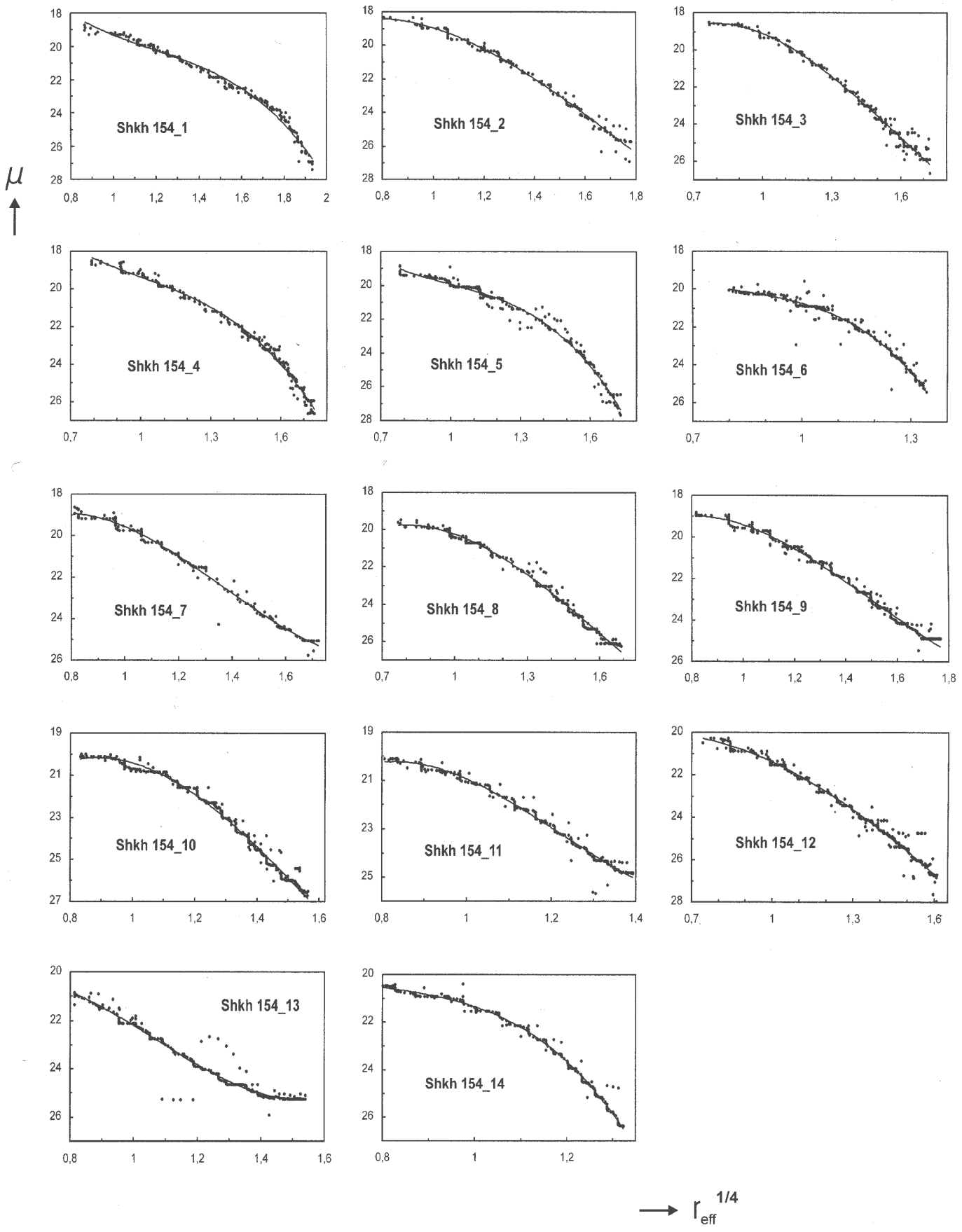

Fig. 5. Surface brightness (in R), μ, vs. effective radius, $r_{\rm eff}^{1/4}$, for the galaxies in ShCG 154.

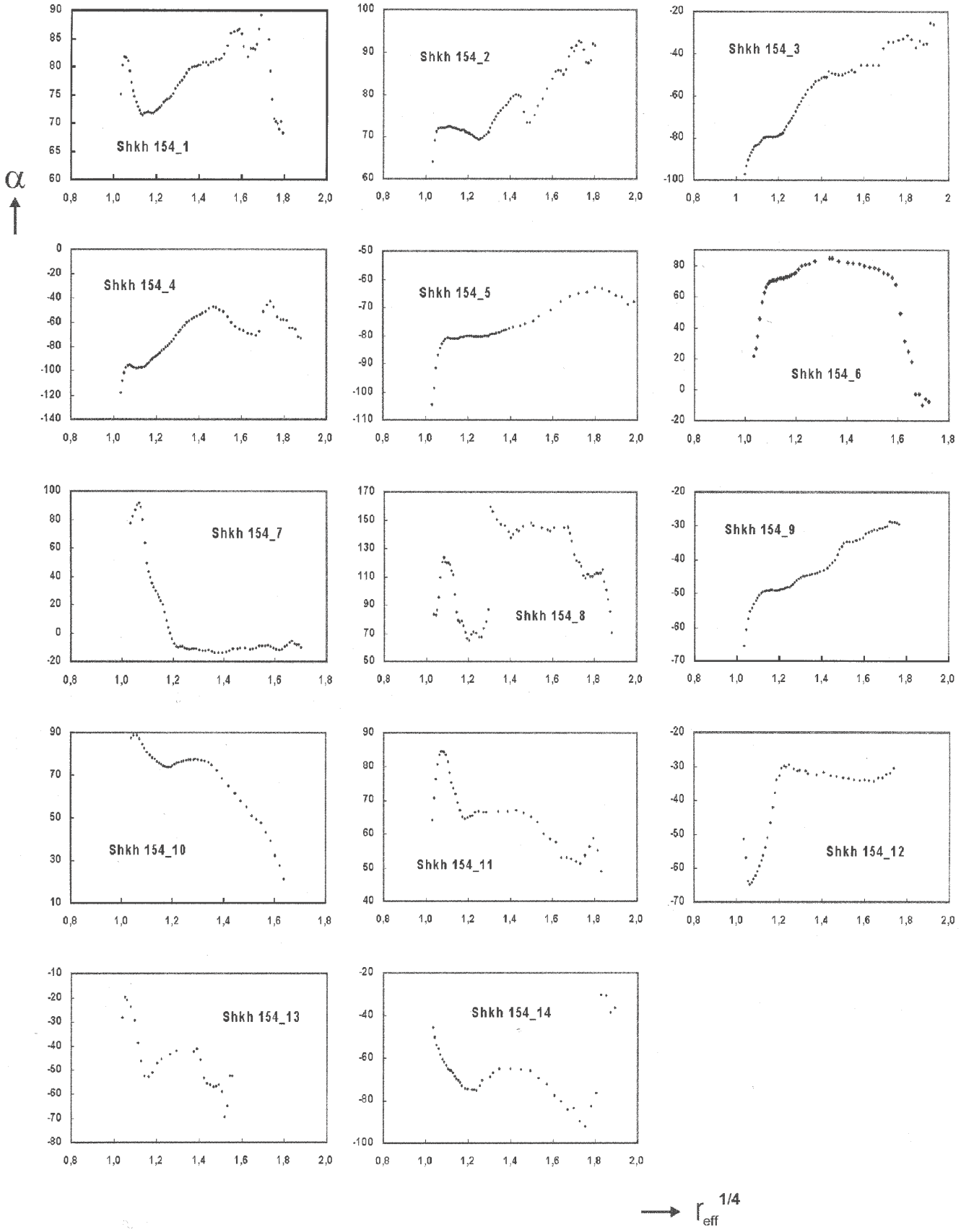

Fig. 6. Position angle α, vs. effective radius, $r_{\rm eff}^{1/4}$, for the galaxies in ShCG 154.

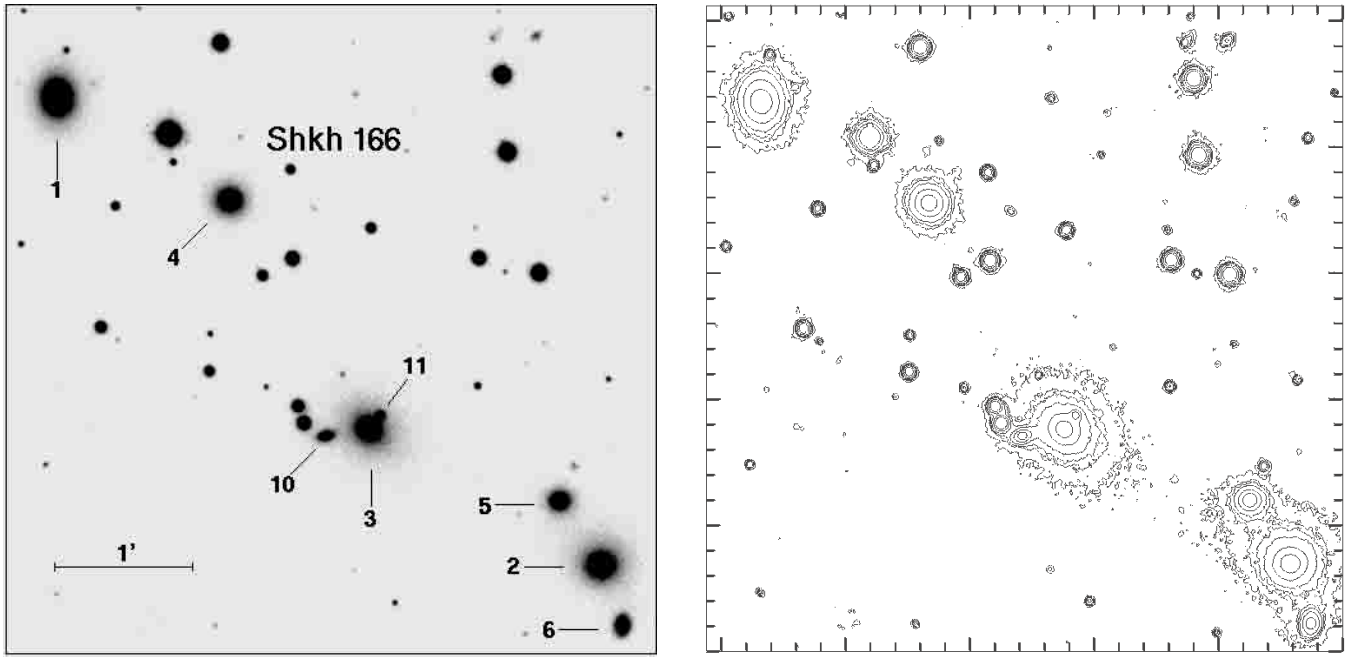

Fig. 7. The photograph of ShCG 166 (left) and the isophotal contour plot of galaxies (right).

Table 5. Photometric parameters of galaxies in ShCG 166.

$g-xy$	B			V			R					type
	m	b/a	D [″]	m	b/a	D [″]	m	b/a	D [″]	α [°]	i [°]	
1	16.10	0.8	25	14.90	0.8	42	13.72	0.8	42	−4	30	S0
2	16.43	0.9	23	15.34	0.8	33	14.23	0.8	28	46	20	S0
3	16.22	0.7	36	15.30	0.7	41	14.43	0.8	42	31	26	S0
4	16.53	0.9	21	15.42	0.9	30	14.38	0.9	31	30	16	E
5	17.00	0.9	18	15.95	0.9	29	14.97	0.8	28	35	23	E
6	17.44	0.8	19	16.48	0.8	27	15.58	0.7	24	−5	28	S0/Sa
10	18.26	0.6	16	17.00	0.6	21	15.91	0.6	21	−75	39	S0/Sa
11	18.38	0.9	11	17.80	0.9	11	17.33	0.9	4	47	21	E

3.3. ShCG 328

This group has the highest galaxy density among the studied four ShCGs. It demonstrates an extreme sign of interaction and, perhaps, merging. The group consists of one bright galaxy 6, and a few fainter objects. Radial velocities of the six brightest members are measured. All have accordant redshifts.

The contour plot (Fig. 10) shows that two central large galaxies, 4 and 6, are embedded in a common extended halo. The most luminous of them, galaxy 6, has apparently undergone disruption by tidal heating: its radius in R reaches about 50 kpc at a surface brightness $\mu = 25^{\rm m}/{\rm arcsec}^2$. Both these galaxies have faint and compact companions in their immediate neighbourhood (galaxy 5, and galaxies 7 and 10, respectively). Interestingly, both galaxies show also a disturbation in the twisting curve. Membership of the latter galaxies to the group is not proved spectroscopically. Consideration of direct images shows, however, that compact galaxies 5 and 7 are, possibly, interacting with their brighter companions. The luminosity profiles $\mu - r_{\rm eff}^{1/4}$ show that both galaxies have very small sizes. They seem to be stripped out of halos. At the same time, they are much brighter on the R image (compare them to two background galaxies north of galaxy 3 on the left panel of Fig. 10). Apparently, as in the case of galaxy 11 in ShCG 166, these galaxies seem to have lost their halos as a result of gravitational influence of the corresponding bright neighbours. The same, probably, applies to galaxy 10.

Galaxy 3 is touching the common extended envelope of the central two bright galaxies of the group. Its extended halo is, possibly, a sign of interaction with galaxies 4 and 6.

Galaxies 1, 2, 8, and 9 are far from the group center, and their halos seem to be undisturbed, only the twisting curves of galaxies 2 and 8 suggest tidal perturbations. The membership of galaxy 9 of the group is not certain; we do not have its redshift.

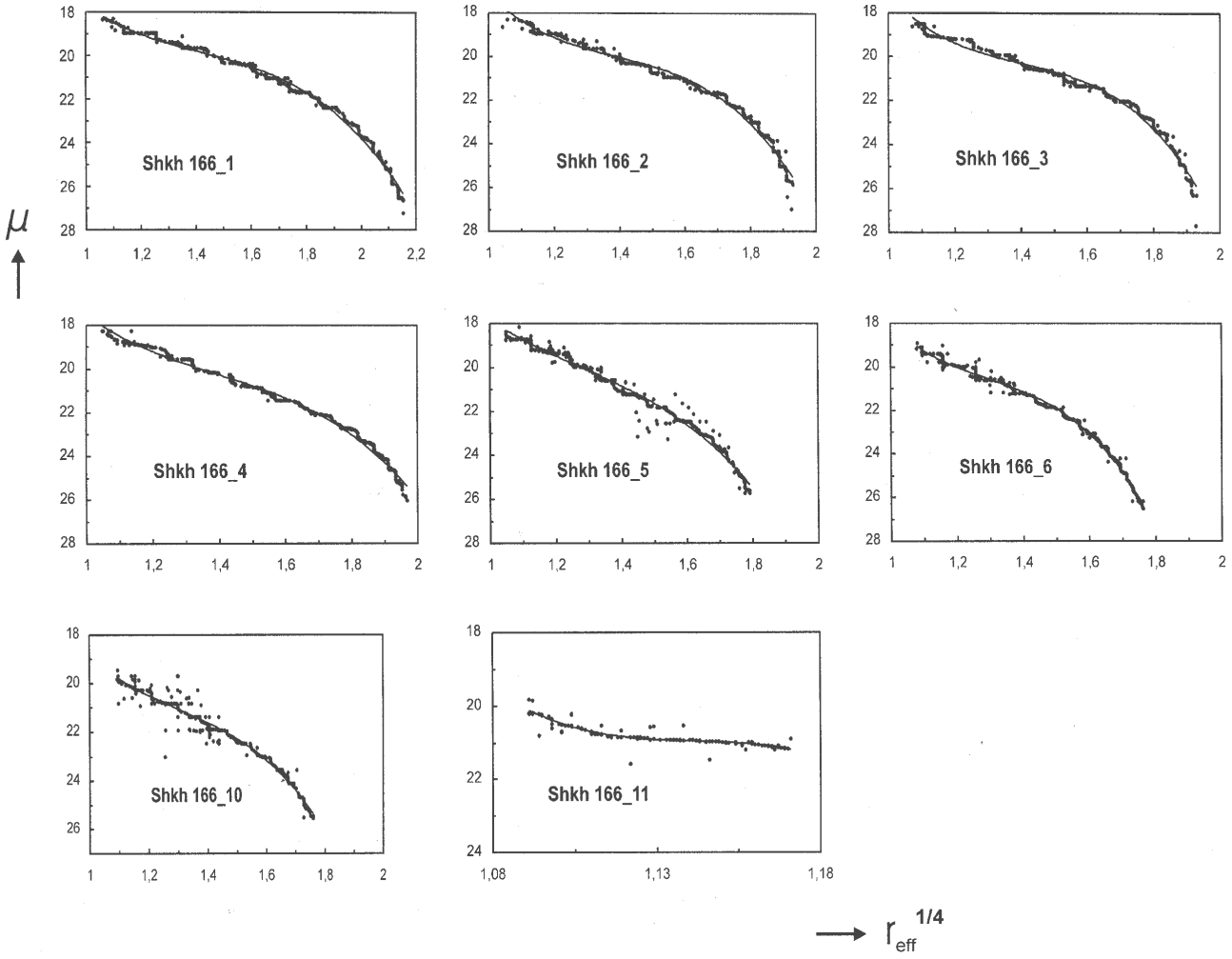

Fig. 8. Surface brightness (in R), μ, vs. effective radius, $r_{\rm eff}^{1/4}$, for the galaxies in ShCG 166.

The group consists of E/S0 type galaxies with only one exception – galaxy 1, which was classified as Sa. It is located at the periphery of the group, and obviously is not interacting with other galaxies. Also, its RV has the largest difference from the mean value of the group.

The $\mu - r_{\rm eff}^{1/4}$ profiles of the surface brightness in R versus effective radius for galaxies in the studied group are presented in Fig. 11. The twisting curves α vs. $r^{1/4}$ are seen in Fig. 12.

3.4. ShCG 360

All eight spectroscopically observed galaxies have accordant redshifts. This group is the central part of the cluster A2113, and is well isolated from the other members of the cluster.

The contour plot (right panel of Fig. 13) shows that the two brightest galaxies 1 and 14 are certainly interacting with each other. Galaxy 1 has radio emission (Tovmassian et al. 1999), which is a hint of the ongoing interaction. Galaxy 5 seems also to be engaged in interaction, because its inner isophotes are extended (in comparison to undisturbed galaxies, e.g. galaxy 8), and this galaxy has also a disturbed twisting curve. Moreover, it has an elongation towards galaxy 1. One may get an impression that galaxies 2, 3 and 4 are also embedded in the common large diffuse halo, and the twisting profiles show signs of disturbations, too. However, the outermost isophotes of other galaxies of the group, which apparently are not in interaction, e.g. 7, 8, 10, and of the other fainter ones, are also sufficiently large. If galaxies 2, 3 and 4 have similar large halos, overlapping of their images with the very extended common halo of the central two galaxies may give an impression of interaction of these galaxies with the latter two. Similarly, galaxies 6, 9, 12, 13 and 15 may be also just projected over the large halo of the central two galaxies. Redshifts of galaxies 6, 12, and 13 are not measured, and their membership of the group is not confirmed.

Only three galaxies, 3, 8 and 11, out of 15 are of S0/Sa type. All three galaxies are located around the large central envelope, and one of them, 3, seems to be at initial stage of interaction.

The $\mu - r_{\rm eff}^{1/4}$ profiles of the surface brightness in R versus effective radius for galaxies in the studied group are presented in Fig. 14. The twisting curves α vs. $r^{1/4}$ are seen in Fig. 15.

3.5. Physical parameters of the studied groups

The results of the photometry of member galaxies in the studied groups, and the knowledge of distances of groups allowed us to deduce physical parameters of groups presented in Table 8.

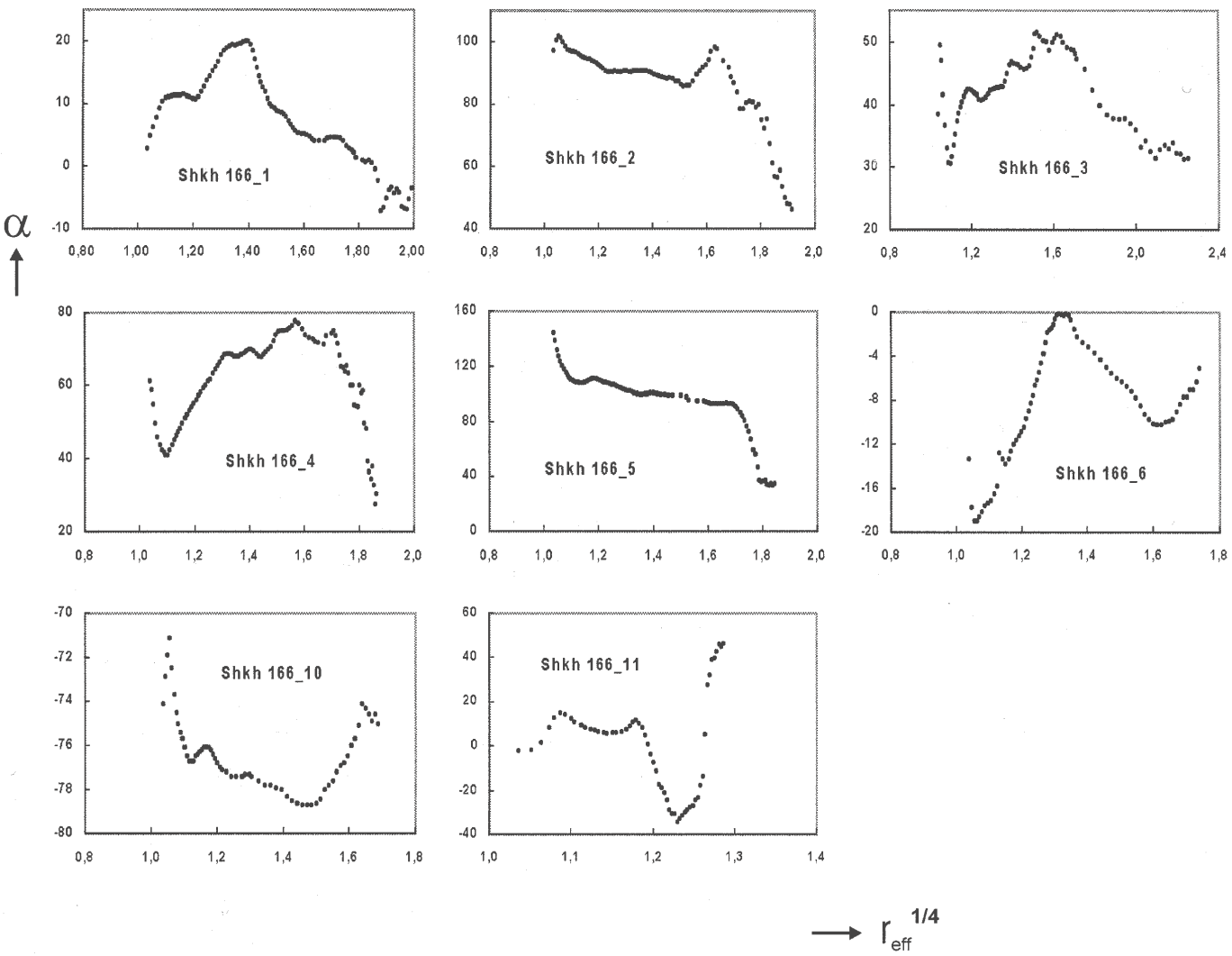

Fig. 9. Position angle, α, vs. effective radius, $r_{\rm eff}^{1/4}$, for the galaxies in ShCG 166.

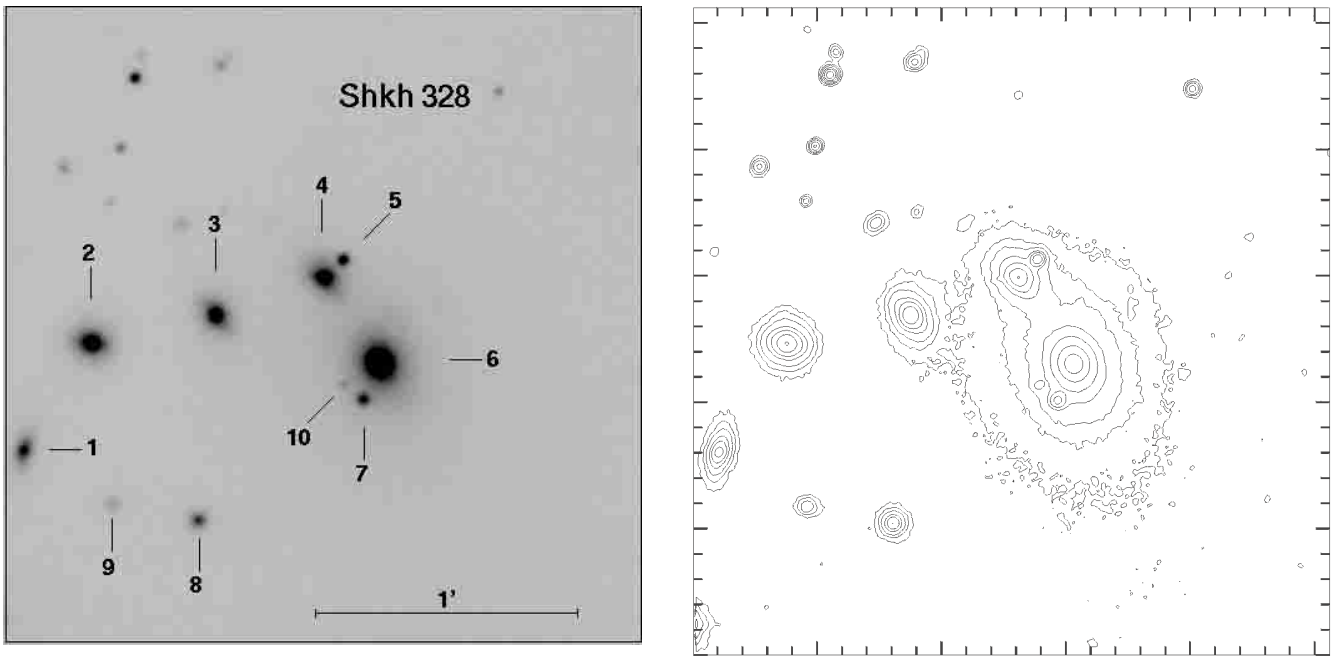

Fig. 10. The photograph of ShCG 328 (left) and the isophotal contour plot of galaxies (right).

Table 6. Photometric parameters of galaxies in ShCG 328.

$g-xy$	B			V			R					type
	m	b/a	D [″]	m	b/a	D [″]	m	b/a	D [″]	α [°]	i [°]	
1	17.74	0.7	14	16.90	0.7	16	15.86	0.8	22	−14	50	Sa
2	17.20	0.9	14	16.14	0.9	18	14.91	0.8	24	77	20	E
3	17.46	0.8	16	16.26	0.8	20	14.92	0.8	35	10	32	E
4	17.48	0.7	16	16.27	0.8	19	15.11	0.7	30	46	32	E/S0
5	18.61	0.8	10	17.77	0.8	11	16.82	0.9	10	−61	35	E
6	15.88	0.7	27	14.35	0.9	30	12.93	0.8	85	16	32	E
7	19.05	0.6	13	17.93	0.9	14	17.01	0.9	14	−64	21	E/S0
8	18.88	0.9	11	17.82	0.8	14	16.71	0.9	17	−69	29	E/S0
9	19.85	0.8	10	19.07	0.9	11	18.17	0.8	11	81	32	S0

Table 7. Photometric parameters of galaxies in ShCG 360.

$g-xy$	B			V			R					type
	m	b/a	D [″]	m	b/a	D [″]	m	b/a	D [″]	α [°]	i [°]	
1	18.10	0.8	14	16.90	0.8	19	15.74	0.8	20	9	35	S0
2	18.13	0.9	12	17.13	0.8	16	16.06	0.8	16	43	29	S0
3	18.28	0.7	12	17.43	0.6	16	16.32	0.7	16	−63	25	S0/Sa
4	19.44	0.7	8	18.32	0.7	13	16.97	0.7	15	11	20	S0
5	18.96	0.8	12	17.98	0.8	16	16.58	0.9	16	11	18	S0
6	20.02	0.8	8	18.47	0.8	12	17.08	0.9	13	35	30	E/S0
7	19.62	0.9	11	18.35	0.9	13	17.17	0.9	14	72	20	S0
8	19.56	0.8	10	18.40	1.0	13	17.22	0.9	15	39	28	S0/Sa
9	19.80	0.6	9	18.78	0.7	12	17.51	0.6	12	46	25	S0
10	19.33	0.7	11	18.08	1.0	14	16.93	0.9	14	80	29	S0
11	20.24	0.7	9	19.08	0.8	11	18.00	0.8	12	−59	27	S0/Sa
12	19.22	0.9	13	18.38	0.9	15	17.07	0.9	15	9	27	E
13	19.29	0.9	9	18.84	0.9	10	17.78	0.9	12	−30	8	S0
14	18.08	0.9	15	17.10	0.9	17	15.81	0.8	19	29	27	E/S0
15	20.09	0.7	8	18.73	0.8	12	17.09	0.8	18	51	21	E

In the consecutive lines of it the following information is given: line 1 – the redshift, z, weighted by masses of member galaxies; line 2 – the distance, d, of the group (H = 55 km s^{-1} Mpc^{-1}); line 3 – the projected diameter of the group, D; line 4 – the radial velocity dispersion (RVD), σ_v, weighted by masses of galaxies; line 5 – the virial radius, R_{vir}, of the group weighted by masses of galaxies; line 6 – the virial mass, $\mathcal{M}_{vir}$; line 7 – the luminosity of the group, L, in solar units; line 8 – the mass-to-luminosity ratio in solar units, $\mathcal{M}_\odot/L_\odot$; line 9 – the crossing time, τ_c.

The RVDs of the groups are deduced by weighting by masses of galaxies, since in groups with small number of members the differences between the weighted and unweighted RVDs may reach a factor of ∼2. The weighting is made according to the formula:

$$\sigma_v^2 = \mathcal{M}_{tot}^{-1} \sum (\mathcal{M}_i \Delta v_i^2).$$

$\mathcal{M}_{tot}^{-1}$ is the sum of the masses of all the individual spiral and elliptical galaxies of the group estimated using the corresponding V magnitudes and adopting a mass-to-luminosity ratio of 4 and 8 respectively (Karachentsev 1987).

Table 8. The physical parameters of the studied ShCGs.

Parameter	ShCG 154	ShCG 166	ShCG 328	ShCG 360
z	0.0730	0.0396	0.0456	0.1082
d [Mpc]	400	215	250	590
D [kpc]	260	420	95	190
σ_v [km s^{-1}]	215	135	130	260
R_{vir} [kpc]	100	125	40	80
$\mathcal{M}_{vir}$ [10^{11} $\mathcal{M}_\odot$]	49.1	24.1	7.1	57.1
L [$10^{11} L_\odot$]	5.5	4.1	3.0	5.4
$\mathcal{M}/L$ [$\mathcal{M}_\odot/L_\odot$]	8.9	5.8	2.3	10.7
τ_{cr} [10^6 a]	190	380	120	130

The RVDs of all four groups are comparable to the typical value of about 200 km s^{-1} of the HCGs (Hickson et al. 1992), and LGs (Geller & Huchra 1983), though the RVDs of groups ShCG 154 and ShCG 360 are slightly higher than the typical value for compact groups[4]. Anyhow, they are much less than

[4] Both groups are poor galaxy clusters, A1238 and A2113, respectively.

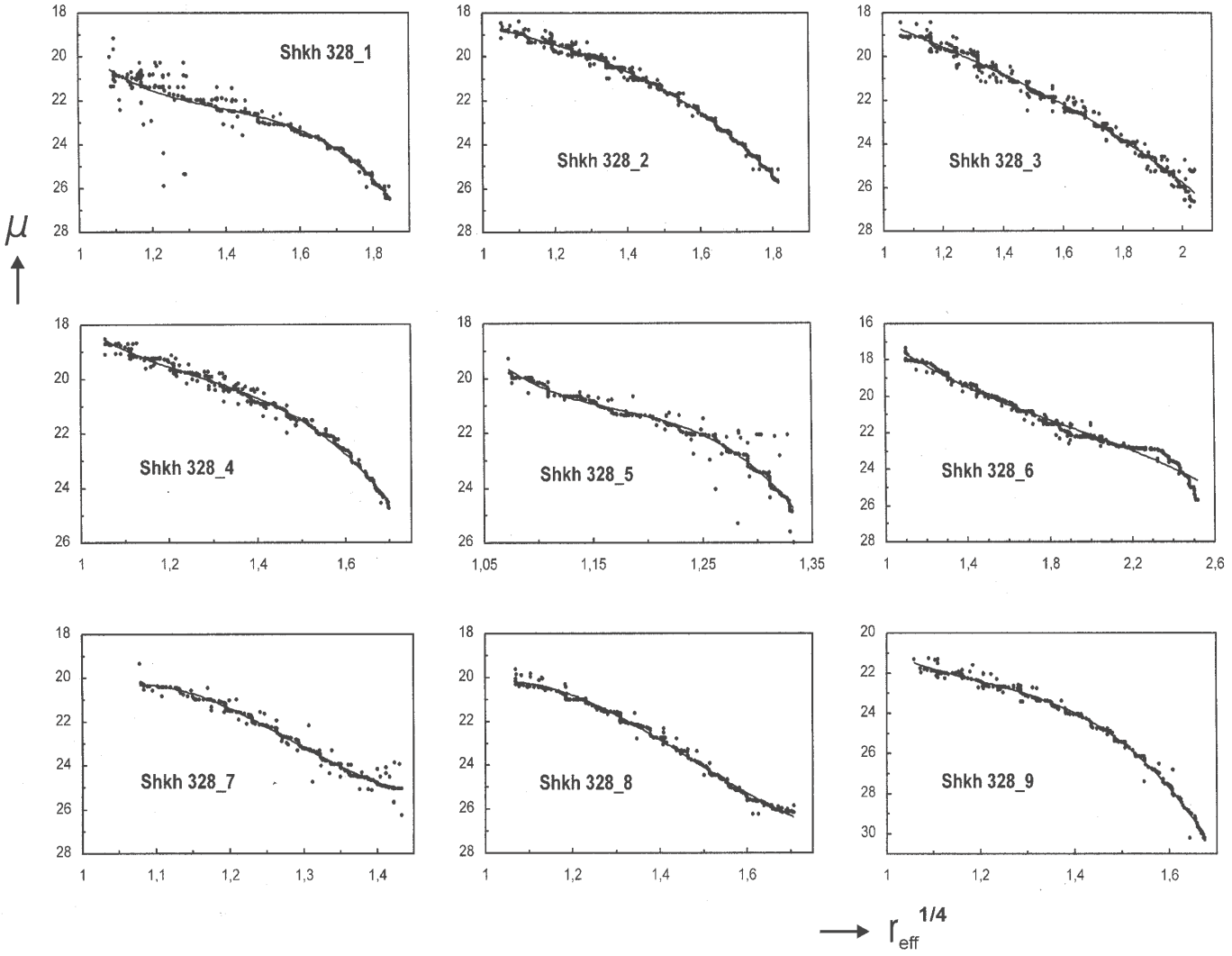

Fig. 11. Surface brightness (in R), μ, vs. effective radius, $r_{\rm eff}^{1/4}$, for the galaxies in ShCG 328.

the typical RVD of rich galaxy clusters of about 1000 km s^{-1} (Zabludoff et al. 1990).

The evolution of CGs depends obviously on the amount of mass, the galaxy distribution in it, and the crossing time. We estimated the masses of groups using the Virial theorem:

$$\mathcal{M}_{\rm vir} = 3\pi\sigma_{\rm v}^2 R_{\rm vir} G^{-1},$$

where

$$R_{\rm vir} = \mathcal{M}_{\rm tot}^2 \left[\sum \mathcal{M}_i \mathcal{M}_j / R_{ij}\right]^{-1}.$$

The estimated virial masses of groups reach $\sim 6 \times 10^{12}$ $\mathcal{M}_\odot$. The derived mass of a group has some uncertainty because of unknown projection effects which become important in the case of small number of galaxies. However, the obtained values are typical for galaxy groups, and do not exhibit extreme fluctuations.

The mass-to-luminosity ratios for ShCGs were obtained from the estimated Virial masses and the total luminosities of corresponding groups. The latter were estimated by using the V magnitudes of individual galaxies. The mass-to-luminosity ratios cover a range from 2 to 11. The $\mathcal{M}/L$ ratios for ShCGs are comparable to the dynamical $\mathcal{M}/L$ ratio of ~8 for ellipticals (Karachentsev 1987). It means that the amount of dark matter in these four ShCGs is nearly identical to the dark matter of its members.

The crossing time was estimated according to the formula (Gott et al. 1973):

$$\tau_{\rm cr} = (3/5)\pi/2R_{\rm vir}(\sqrt{3}\sigma_{\rm v})^{-1}.$$

For the four ShCGs $\tau_{\rm cr}$ range from 120 to 380×10^6 years.

3.6. The physical state of ShCGs

We measured BVR magnitudes of 46 galaxies. Only four galaxies (ShCG 154-6, ShCG 154-12, ShCG 166-11, and ShCG 360-13) are bluer than $B - V = 0.8$ (see Tables 4, 5, 7). Galaxy ShCG 154-12 is, possibly, a spiral in the outskirts of the group. The other two blue galaxies, ShCG 154-6 and ShCG 166-11 are classified as E/S0 and E types respectively, and their blue color seems suspicious. Both galaxies are interacting with much brighter neighbours. The B magnitudes of these galaxies are measured with sufficiently high accuracy, while the V magnitudes may be contaminated by the

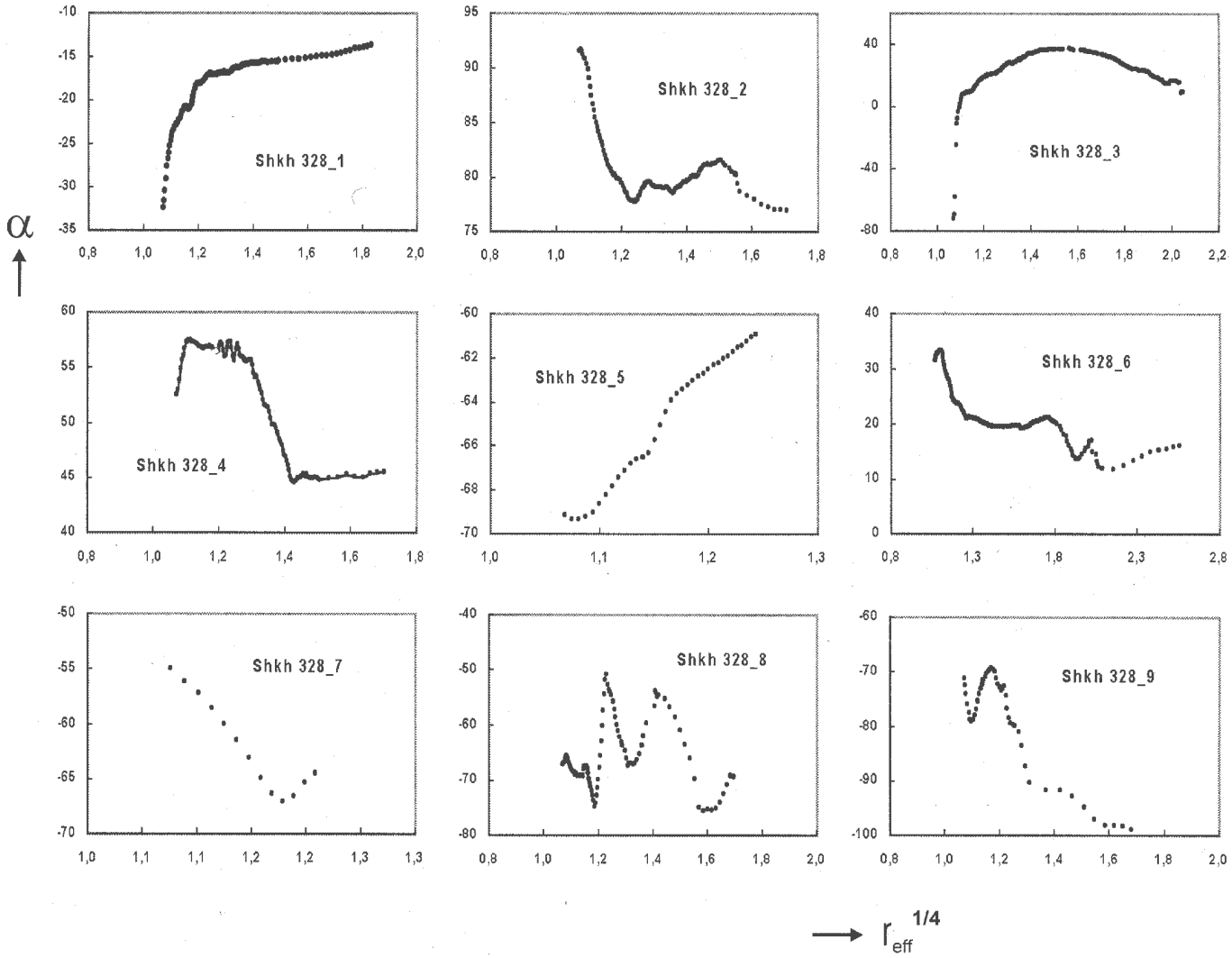

Fig. 12. Position angle, α, vs. effective radius, $r_{\rm eff}^{1/4}$, for the galaxies in ShCG 328.

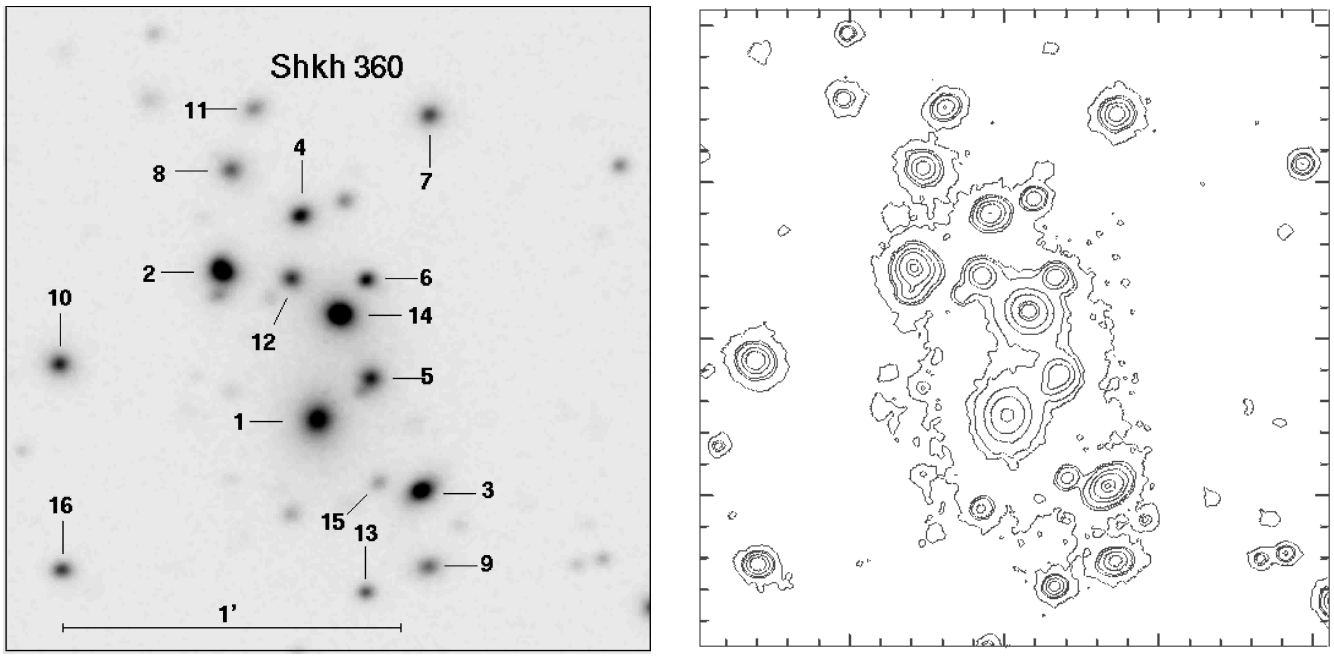

Fig. 13. The photograph of ShCG 360 (left) and the isophotal contour plot of galaxies (right).

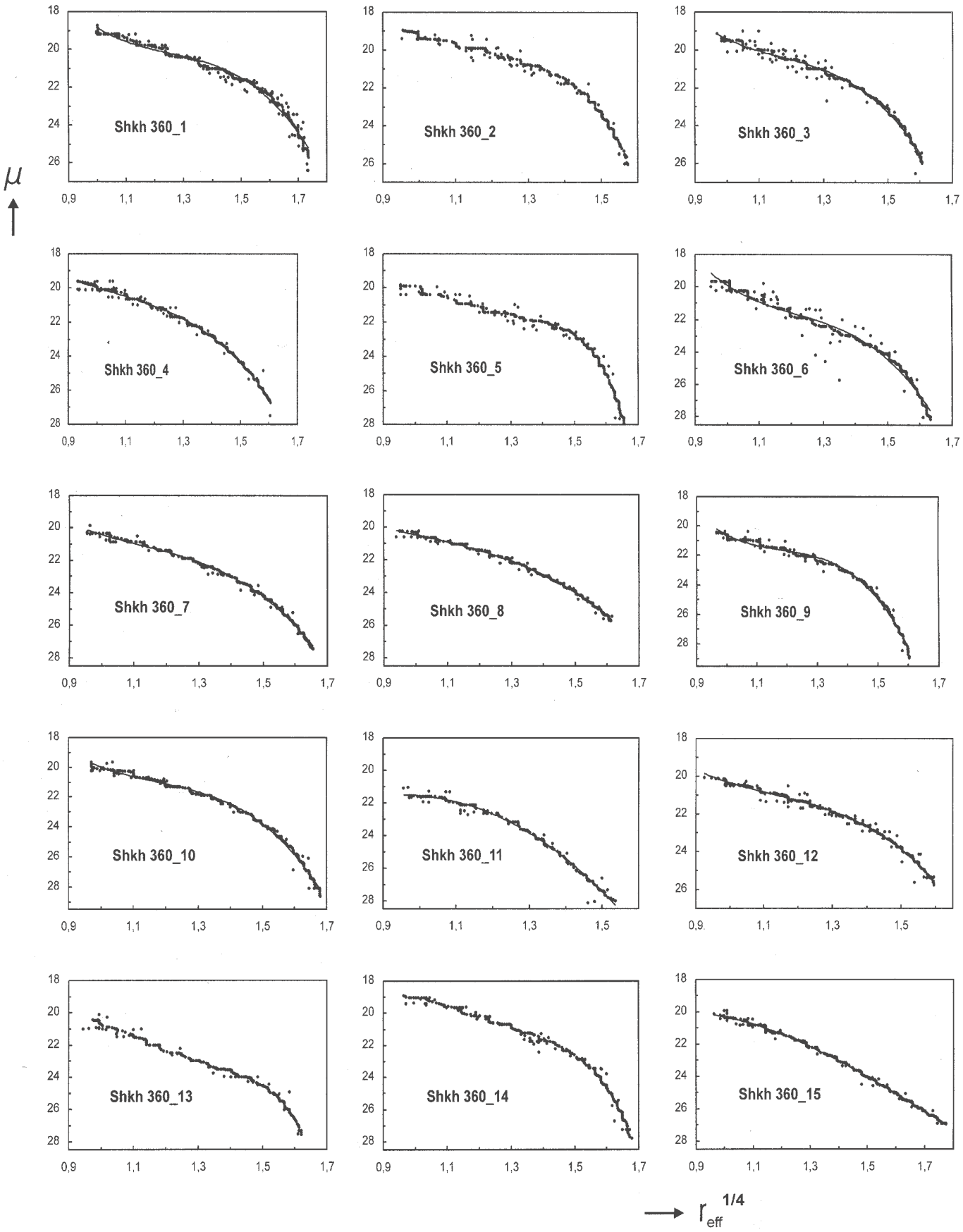

Fig. 14. Surface brightness (in R), μ, vs. effective radius, $r_{\rm eff}^{1/4}$, for the galaxies in ShCG 360.

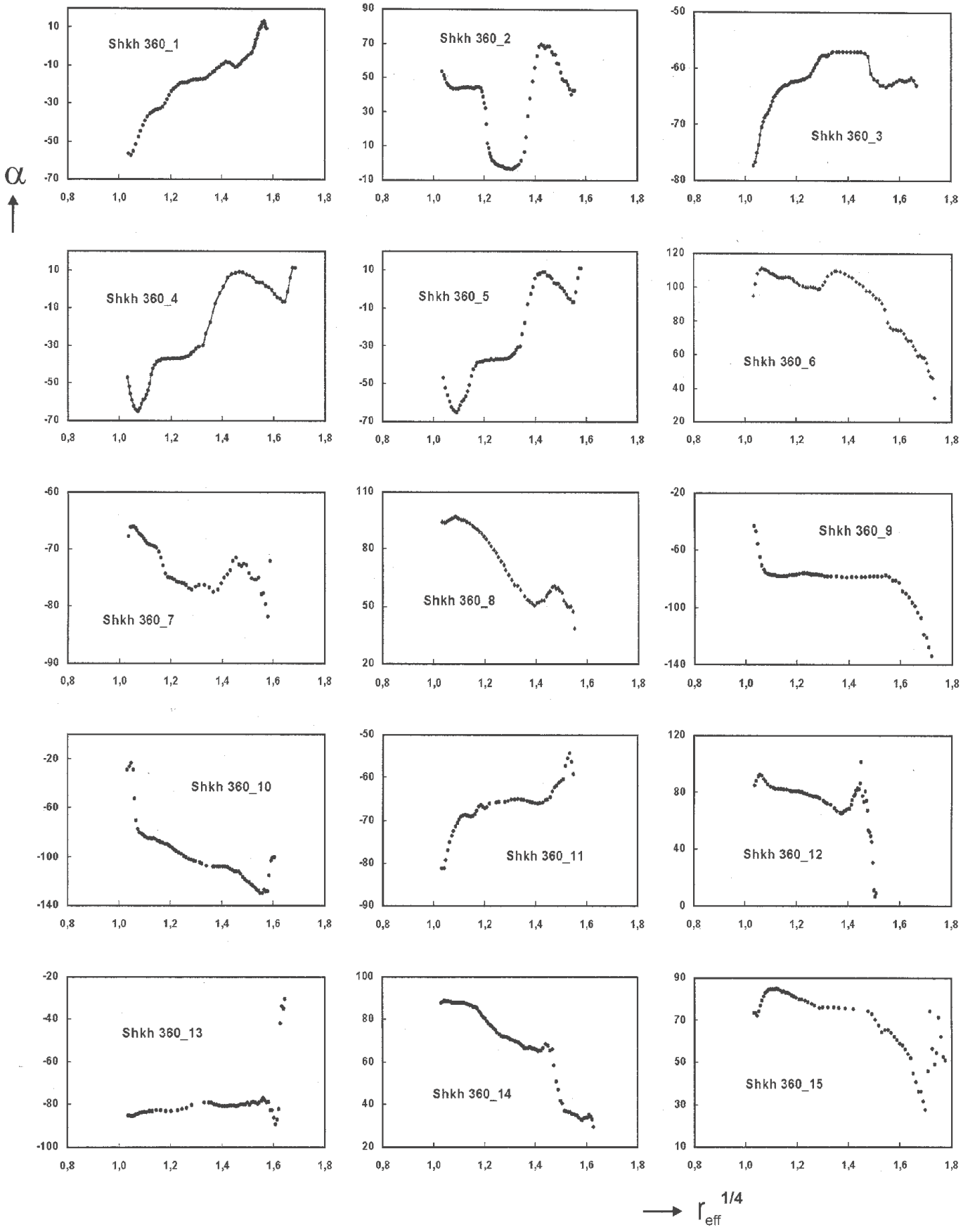

Fig. 15. Position angle, α, vs. effective radius, $r_{\rm eff}^{1/4}$, for the galaxies in ShCG 360.

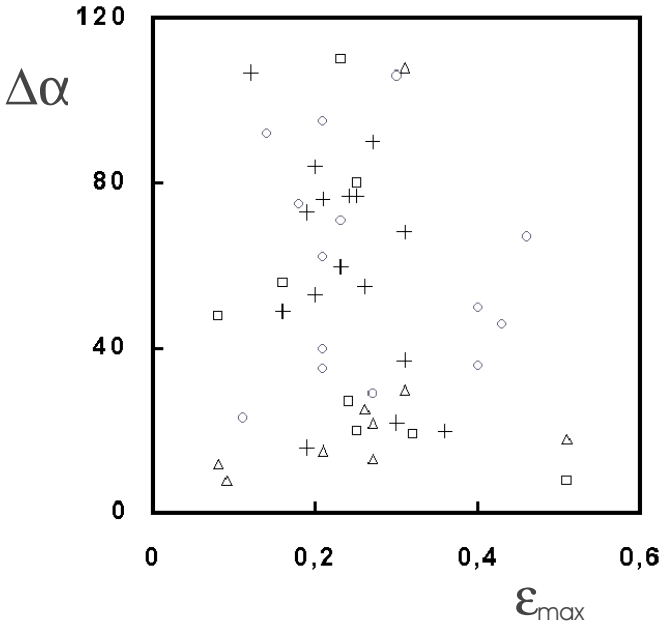

Fig. 16. Correlation between the maximum isophotal twisting, $\Delta\alpha$, vs. maximum ellipticity, $\varepsilon_{\max}$, for the galaxies in the group ShCG 154 – circles, ShCG 166 – squares, ShCG 328 – triangles, and ShCG 360 – crosses.

large extended halo of the neighbour galaxies in which they are embedded. There are no emission lines in the spectrum of galaxy ShCG 166-11. Hence, its blue colour is not due to a starburst. The radial limits of the isophotal shapes of galaxy ShCG 166-11 in B and R are different. It is obvious that its R magnitude is underestimated. The same is true for ShCG 154-6 as well. For this reason their $B - V$ magnitudes may not be reliable. Galaxy ShCG 360-13 is an elliptical. Its membership to the group is not proved spectroscopically.

Thus, we revealed mainly red galaxies in the studied four ShCGs. A population of bright blue elliptical galaxies, predicted by models of evolution of galaxies, is missed here. This result confirms the finding of Zepf et al. (1991) of a very small number of blue ellipticals in CGs. Possibly the environment dominated models that predict a larger frequency of blue ellipticals due to interactions and mergers have to be modified.

None of the four ShCGs has measurable FIR emission (Tovmassian et al. 1999).

Accepting the idea that the structure of early-type galaxies is the result of the combined effects during the epoch of galaxy formation and of subsequent environmental processes as e.g. close encounters or mergers, we investigated the twisting of isophotes in the galaxies of the Shakhbazian groups to look for tidal effects. This twisting is reflected in Fig. 16 that shows the classical correlation between the maximum isophotal twisting and the maximum ellipticity (Galletta 1980). In this figure the galaxies of the four Shakhbazian groups have been indicated with different symbols: ShCG 154 – circles, ShCG 166 – squares, ShCG 326 – triangels, and ShCG 360 – crosses. Figure 16 shows that the galaxies are distributed over a wide range of $\Delta\alpha$, whereas the majority of them is concentrated around $\varepsilon_{\max} \sim 0.2$. This result resembles the finding of Fasano & Bonoli (1989), Rampazzo & Buson (1990) and Fasano & Bettoni (1994). According to the scenario that tidal perturbations play a dominant role in determining the structure of the galaxies, a large number of twisted galaxies should be expected in the Shakhbazian compact galaxy groups. To be compatible with Galleta (1980) and Rampazzo & Buson (1990) we also divided our sample into a set of objects with α lower than 10° (apparently untwisted objects) and a second one with α greater than 10° (twisted objects). Interestingly, an isophotal twisting lower than 10° is found only in two objects (ShCG 166-10, ShCG 328-5), i.e. in less than 10% of the objects. This finding, that more than 90% of the galaxies are twisted objects (in the sample of Fasano & Bonoli 1989 and Rampazzo & Buson 1990 the twisting is present in ∼70% of the early-type galaxies) may be interpreted as the result of strong tidal interactions in the environment of a high galaxy density typical for the Shakhbazian compact galaxy groups.

Looking in detail at the distribution of $\Delta\alpha$ for the four Shakhbazian groups we find that the obviously most evolved galaxy group ShCG 328 (△) shows a relatively small variation in $\Delta\alpha$ compared to the other groups. Provided this finding is not only a result of a statistics with a small number of objects it may be interpreted in the following manner: a) in evolved groups the twisting is smoothed in enlarged halos of galaxies or b) the tidal effects play only a limited role in determining the structure of early-type galaxies (what contradicts to the 90%–level of twisted objects in the four groups).

The problem of the correlation between the presence of optical signs of galaxy-galaxy interaction and the presence of hot X-ray emitting intragroup gas has been intensively discussed in the literature. An optical property that predicts the presence of the X-ray emission is the large elliptical fraction (Ebeling et al. 1994). Interactions and merging of galaxies play a major role in the morphology of galaxies (Toomre & Toomre 1972). Such processes should be very effective in the dense environment of CGs. As a consequence of interactions, the gas in galaxies is heated and is expelled into the intragroup medium by tidal effects and ram pressure. Thus, spirals lose their gas content, and convert to S0/E types. Hence, the rate of spirals should be small in CGs. The minority of late type galaxies in the ShCGs is remarkable. There is only one galaxy of Sa type, ShCG 328-1, and nine galaxies are classified as S0/Sa. If all of them are spirals then the spiral rate in the studied four ShCGs is ∼22%. Hence, these ShCGs are dynamically more evolved than HCGs the spiral rate in which is about half the population (Hickson et al. 1989a). Because of the limited number of galaxies within a CG it is very unlikely that the gas injection rate into the intragroup medium is stable enough to maintain the X-ray source in the steady-state. It means that different stages of interaction should be traced by the extended X-ray emission caused by thermal bremsstrahlung from the hot intracluster medium (ICM). The least interacting group ShCG 166 (Fig. 7) has no measurable X-ray emission. The other three groups with clear signs of interaction have significant extended X-ray emission. Different shapes of the X-ray contour plots possibly indicate different stages of interaction and merging processes. According to N-body simulations with inclusion of intra-cluster gas (Schindler & Müller 1993), in the first stage

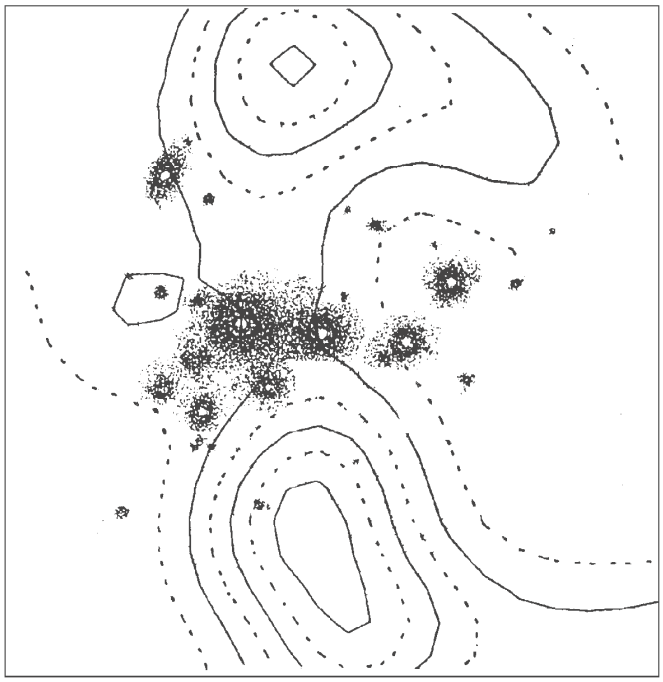

Fig. 17. The contour map of the diffuse X-ray emission of ShCG 154 in arbitrary units. The first contour rate represents X-ray emission at 3 σ with increments of 0.2 σ.

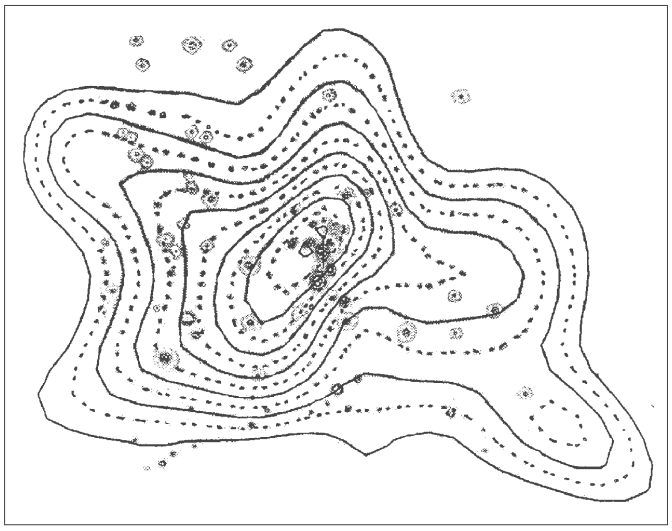

Fig. 18. The contour map of the diffuse X-ray emission of ShCG 360 in arbitrary units. The first contour rate represents X-ray emission at 3 σ with increments of 0.2 σ.

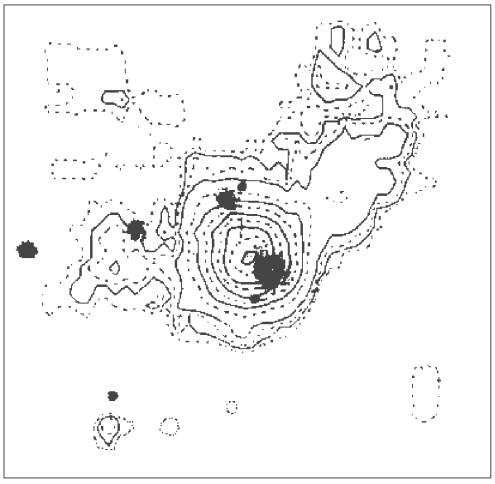

Fig. 19. The contour map of the diffuse X-ray emission of ShCG 328 in arbitrary units. The first contour rate represents X-ray emission at 3 σ with increments of 0.2 σ.

of interaction the ICM is ejected from the cluster orthogonal to the direction of collision. This asymmetric supersonic gas ejection is demonstrated by the resulting lens-shaped shock fronts. An example of this scenario is ShCG 154 (Fig. 17), where two hot gas lobes are observed. This group has also radio lobes (Owen et al. 1992) in the same direction. Obviously the hot luminous gas is extending beyond the optically visible group. After the violent shock stage, the ICM reaches a quasi-equilibrium stage with an almost spherically symmetrical density distribution, as in ShCG 360 (Fig. 18).

In the late phase of evolution the outer parts of the X-ray emitting regions of galaxy groups may be cooled or diluted by the gas diffusion, and their sizes may be reduced. However, the center of the X-ray emitting region should coincide with the gravitational center of the potential well of the group, as in ShCG 328 (Fig. 19).

The X-ray emission of a galaxy cluster is correlated with the σ_v: $L_X \sim \sigma_v^4$ (Quintana & Melnick 1982). Dell'Antonio et al. (1994) and Ponman et al. (1996) showed that rich groups follow the $L_X \sim \sigma_v^4$ relation, but groups with smaller RVD (<300 km s^{-1}) have a more shallow slope. Mahdavi et al. (2000) showed that the correlation between L_X and σ_v may be best represented by a broken power law with $a \sim 1.4$ for galaxy groups and $a \sim 4$ for galaxy clusters. Figure 20 shows that ShCGs represent the low-mass extension of clusters and have sufficiently large dispersion[5]. In groups only a relatively small amount of X-ray emitting gas is dominated by the global group population, but most of the intragroup gas is concentrated in pools around individual galaxies. Thus, it is assumed that the total observed X-ray flux in groups is a sum of emission from gas in the global group potential and emission of gas concentrated in the environment of individual galaxies. The large dispersion of ShCGs on the $L_X - \sigma$ plot (Fig. 20) may be explained by fact that the measured RVD for CGs deviates from the true RVD: it depends on the orientation of the elongation of the group (Tovmassian et al. 1999; Tovmassian & Tiersch 2001).

[5] The not published results (Tiersch et al., in preparation) on some other X-ray emitting ShCGs are included in Fig. 20.

4. Conclusions

The *RV*s of galaxies in the studied four groups show that all of them with, possibly, one exception, ShCG 154-10, belong to the corresponding groups. The redshifts of the studied four ShCGs cover a range 0.04-0.11. Hence, these groups are located beyond the Local Supercluster. The mass-weighted RVD of four ShCGs ranges between 130 km s^{-1} and

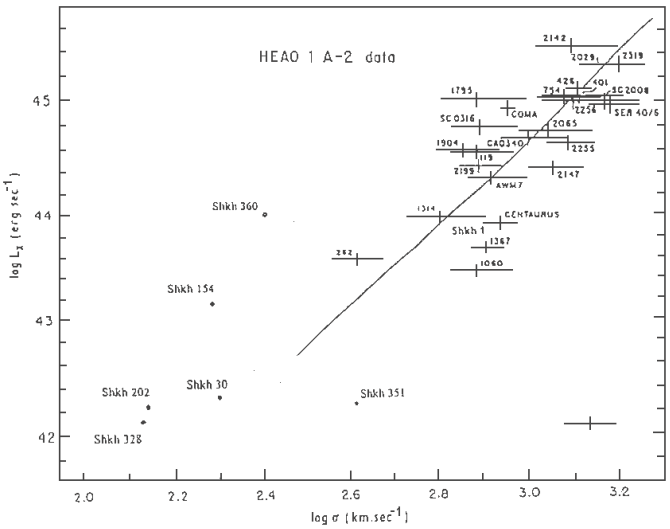

Fig. 20. Correlation between the X-ray luminosity, L_X, and the velocity dispersion, σ_v. The error bar for ShCGs is shown on the lower right of the figure.

260 km s^{-1}, which is comparable to that of HCGs and loose galaxy groups. The virial radius is of the order of 100 kpc; ShCG 328 is an exception with only 40 kpc virial radius. The derived virial masses of these four groups range up to 6×10^{12} $\mathcal{M}_\odot$. These values are typical for galaxy groups. The mass-to-luminosity ratio, deduced from the V magnitude, is within 2 and 11. The $\mathcal{M}/L$ values for the studied four ShCGs are comparable to the $\mathcal{M}/L$ of individual galaxies. This means that these four groups have almost no dark matter. The crossing time for these four ShCGs ranges from 120 to 380 million years. This is much smaller than the Hubble age. It is, however, necessary to take into account that the crossing time deduced from the estimated virial radius and velocity dispersion may, in fact, be larger. Indeed, ShCGs have very elongated "cigar"-like configuration (Oleak et al. 1995, 1998). Member galaxies in them move preferentially in the direction of elongation of the group (Tovmassian & Tiersch 2001). Near the gravitational center of the group the velocities are high enough. Then, the measured velocity dispersion of groups the elongation of which is oriented nearly orthogonal to the line of sight would be smaller than the real values, while the linear sizes of such groups would, on average, be larger than that of those seen almost end-on. As a result, the estimated crossing times of elongated groups may, on average, be higher than that of the round ones.

The ejection of interstellar gas from galaxies by ram pressure and/or tidal forces results in a high percentage of E and S0 galaxies (~75%) in four ShCGs. The hot X-ray emitting intragroup gas is detected in three groups: ShCG 154, ShCG 328, and ShCG 360. It helps to trace the stages of evolution of the hot intra-cluster gas. The measured *RV*s as well as the X-ray emission prove that these four ShCGs are physical entities.

Acknowledgements. Authors are grateful to the anonymous referee for valuable comments. HT is grateful to the Government of the Land Brandenburg for the support of this work (Az 24-19/003; 2000), to the DFG for the grants TI 215/1-1, TI 215/2-1, TI 215/3-1, TI 215/4-1, and to Mr. O. Beck for private financial support. HMT acknowledges the 1997 DAAD grant, the DFG for the project 444Mex 112/2/98, as well as the Königsleiten Observatory for the partial financial support during June-August 2001. SN thanks the DFG for the projects 436 RUS 17/56/95 and 436 RUS 17/64/94. DS acknowledges the support of the DFG, TI 215/7-1. AA thanks the DFG for the grant 436 ARM 17/2/94.

References

Arp, H. 1966, ApJS, 14, 1
Amirkhanian, A. S. 1989, Soobshch. Byurakan Obs., 61, 27
Amirkhanian, A. S., & Egikian, A. G. 1987, Astrofizika, 27, 395
Arp, H. C., Burbidge, G. R., & Jones, T. W. 1973, PASP, 85, 423
Baier, F. W., Petrosian, M. B., Tiersch, H., & Shakhbazian, R. K. 1974, Astrofizika, 10, 327
Baier, F. W., & Tiersch, H. 1975, Astrofizika, 11, 221
Baier, F. W., & Tiersch, H. 1976a, Astrofizika, 12, 7
Baier, F. W., & Tiersch, H. 1976b, Astrofizika, 12, 409
Baier, F. W., & Tiersch, H. 1978, Astrofizika, 14, 279
Baier, F. W., & Tiersch, H. 1979, Astrofizika, 15, 33
Barnes, J. E. 1985, MNRAS, 215, 517
Barnes, J. E. 1989, Nature, 338, 123
Bettoni, D., & Fasano, G. 1993, AJ, 105, 1291
Bettoni, D., & Fasano, G. 1995, AJ, 109, 32
Binggeli, B. 1982, A&A, 107, 338
Bode, P. W., Cohn, N. H., & Lugger, P. M. 1993, ApJ, 416, 17
Coziol, R., Ribeiro, A. L. B., de Carvalho, R. R., & Capelato, H. V. 1998, ApJ, 493, 563
del Olmo, A., & Moles, M. 1991, A&A, 245, 27
Dell'Antonio, I. P, Geller, M. J, & Fabrikant, D. G. 1994, AJ, 107, 427
DiFazio, A., & Flin, P. 1988, A&A, 200, 5
di Tullio, G. A. 1979, A&AS, 37, 591
Duus, A., & Newell, B. 1977, ApJS, 35, 209
Ebeling, H., Voges, W., & Böhringer, H. 1994, ApJ, 436, 44
Fasano, G., & Bettoni, D. 1994, AJ, 107, 1649
Fasano, G., & Bonoli, C. 1989, A&AS, 79, 291
Galletta, G. 1980, A&A, 81, 179
Geller, M. J., & Huchra, J. P. 1983, ApJS, 52, 61
Gott III, J. R., Wrixon, G. T., & Wannier, P. 1973, ApJ, 186, 777
Hasinger, G., Turner, T. J., George, I. M., & Boese, G. 1992, ApJ, OGIP Calibration Memo CAL/ROS/92-001
Hickson, P. 1982, ApJ, 255, 382
Hickson, P., Kindl, E., & Auman, J. R. 1989, ApJS, 70, 687
Hickson, P., Menon, T. K., Palumbo, G. G. C., & Persic, M. 1989, ApJ, 341, 679
Hickson, P., Mendes de Oliveira, C., Huchra, J. P., & Palumbo, G. G. C. 1992, ApJ, 399, 353
Hickson, P. 1993, Astrophys. Lett. Comm., 29, 1
Karachentsev, I. D. 1987, Dvojnye galaktiki (Moskva, Nauka), 76
Kirshner, R. P., & Malamuth, E. M. 1980, ApJ, 236, 366
Kodaira, K., Iye, M., Okamura, S., & Stockton, A. 1988, PASJ, 40, 53
Kodaira, K., Doi, M., Ichikawa, S., & Okamura, S. 1990, Publ. NAO Jpn., 1, 283
Kodaira, K., & Sekiguchi, M. 1991, PASJ, 43, 169
Kormendy, J. 1982, Morphology and Dynamics of Galaxies, ed. L. Mayor, & M. Martinet, Geneva, 113
Lynds, C. R., Khachikian, E. Ye., & Amirkhanian, A. S. 1990, Pis'ma v AZh, 16, 195
Lima Neto, G., & Combes, F. 1993, *N*-body Problem and Gravitational Dynamics, ed. F. Combes, & E. Athonassoula, 181
Mahdavi, A., Böhringer, H, Geller, M. J., & Ramella, M. 1997, ApJ, 483, 68

Mahdavi, A., Böhringer, H, Geller, M. J., & Ramella, M. 2000, ApJ, 534, 114
Mamon, G. A. 1986, ApJ, 307, 426
Mendes de Oliveira, C. 1995, MNRAS, 273, 139
Mirzoyan, L. V., Miller, J. S., & Osterbrock, D. E. 1975, ApJ, 196, 687
Oleak, H., Stoll, D., Tiersch, H., & MacGillivray, H. T. 1995, AJ, 109, 1485
Oleak, H., Stoll, D., Tiersch, H., & MacGillivray, H. T. 1998, Astron. Nachr., 319, 253
Owen, F. N, White, R. A., & Burnes, J. O. 1992, ApJS, 80, 501
Petrosian, M. B. 1974, Astrofizika, 10, 471
Petrosian, M. B. 1978, Astrofizika, 14, 631
Pildis, R. A., Bregman, J. N., & Schomberg, J. M. 1995, AJ, 110, 1498
Ponman, T. J., Bourner, P. D. J., Ebeling, H., & Böhringer, H. 1996, MNRAS, 283, 690
Prandoni, I., Iovino, A., & MacGillivray, H. T. 1994, AJ, 107, 1235
Quintana, H., & Melnick, J. 1982, AJ, 87, 972
Rampazzo, R., & Buson, L. M. 1990, A&A, 236, 25
Robinson, L. B., & Wampler, E. J. 1973, ApJ, 179, L135
Rood, H. J. 1979, ApJ, 233, 21
Rose, J. A. 1977, ApJ, 211, 311
Sandage, A., Freeman, K. C., & Stokes, N. R. 1970, ApJ, 160, 831
Schindler, S., & Müller, E. 1993, A&A, 272, 137
Schlegel, D. J., Finkbeiner, D. P., & Davis, M. 1998, ApJ, 500, 525
Schombert, J. M. 1987, ApJS, 64, 643
Shakhbazian, R. K. 1973, Astrofizika, 9, 495
Shakhbazian, R. K., & Petrosian, M. B. 1974, Astrofizika, 10, 13
Stoll, D., Tiersch, H., Oleak, H., Baier, F., & MacGillivray, H. T. 1993a, Astron. Nachr., 314, 225
Stoll, D., Tiersch, H., Oleak, H., Baier, F., & MacGillivray, H. T. 1993b, Astron. Nachr., 314, 317
Stoll, D., Tiersch, H., Oleak, H., & MacGillivray, H. T. 1994a, Astron. Nachr., 315, 11
Stoll, D., Tiersch, H., Oleak, H., & MacGillivray, H. T. 1994b, Astron. Nachr., 315, 97
Stoll, D., Tiersch, H., & Braun, F. 1996a, Astron. Nachr., 317, 239
Stoll, D., Tiersch, H., & Braun, F. 1996b, Astron. Nachr., 317, 315
Stoll, D., Tiersch, H., & Braun, F. 1996c, Astron. Nachr., 317, 369
Stoll, D., Tiersch, H., & Cordis, L. 1997a, Astron. Nachr., 318, 7
Stoll, D., Tiersch, H., & Cordis, L. 1997b, Astron. Nachr., 318, 89
Stoll, D., Tiersch, H., & Cordis, L. 1997c, Astron. Nachr., 318, 149
Tiersch, H., Oleak, H., Stoll, D., et al. 1995, in Proc. of Fresh Views of Elliptical Galaxies, ASP Conf. Ser. 86 (San Francisco, ASP), ed. A. Buzzoni, A. Renzini, & A. Serrano, 89
Tiersch, H., Oleak, H., Stoll, D., et al. 1995, Max-Planck-Report, 261, 125
Tiersch, H., Oleak, H., Stoll, D., et al. 1995, Astrofizika, 38, 688
Tiersch, H., Oleak, H., Stoll, D., et al. 1996a, in Proc. of From Stars to Galaxies, ASP Conf. Ser. 98 (San Francisco, ASP), ed. C. Leitherer, U. Fritze, V. Alvensleben, & J. Huchra, 523
Tiersch, H., Stoll, D., Neizvestny, S., Tovmassian, H. M., & Navarro, S. 1996b, J. Korean Astron. Soc., 29, 59
Tiersch, H., Stoll, D., Neizvestny, S., Amirkhanian, A., & Mendes de Oliveira, C. 1999, in Proc. of Observational Cosmology: The development of galaxy systems, ed. G. Giuricin, M. Mezetti, & P. Salucci (San Francisco, APS), ASP Conf. Ser., 176, 127
Tiersch, H., Stoll, D., Neizvestny, S., Amirkhanian, A. S., & Egikian, A. G. 1999, in Proc. of Active galactic nuclei and related phenomena, ed. Y. Terzian, D. Weedman, & E. Khachikian (Dordrecht, Kluwer), IAU Symp., 194, 394
Tonry, J., & Davis, M. 1979, AJ, 84, 1511
Toomre, A., & Toomre, J. 1972, ApJ, 178, 623
Tovmassian, H. M. 2001, PASP, 113, 543
Tovmassian, H. M., Mazzarella, J. M., Tovmassian, G. H., Stoll, D., & Tiersch, H. 1998, A&AS, 130, 207
Tovmassian, H. M., Chavushyan, V. H., Verkhodanov, O. V., & Tiersch, H. 1999, ApJ, 523, 87
Tovmassian, H. M., Martinez, O., & Tiersch, H. 1999, A&A, 348, 693
Tovmassian, H. M., & Tiersch, H. 2001, A&A, in press
Vorontsov-Velyaminov, B. A. 1959, Atlas and Catalogue of Interacting Galaxies, vol. I
Yun, M. S., Verdes-Montenegro, L., del Olmo, A., & Perea, J. 1997, ApJ, 475, L21
Zabludoff, A. J., Huchra, J. P., & Geller, M. J. 1990, ApJS, 74, 1
Zepf, S. E., Carvalho, R. R. de., & Ribeiro, A. L. 1997, ApJ, 488, L11
Zepf, S. E., Whitmore, B. C., & Levison, H. F. 1991, ApJ, 383, 524
Zepf, S. E. 1993, ApJ, 407, 448